scientific reports

Check for updates

OPEN

The first sauropod dinosaur from the Lower Cretaceous Khok Kruat Formation of Thailand enriches the diversity of somphospondylan titanosauriforms in southeast Asia

Thitiwoot Sethapanichsakul[1,6], Sasa-On Khansubha[2,6], Sita Manitkoon[3,4]✉, Rattanaphorn Hanta[5], Philip D. Mannion[1] & Paul Upchurch[1]

Sauropod dinosaur remains comprise the majority of the Mesozoic vertebrate fossil record in Thailand. However, they are rare and fragmentary in the Aptian–Albian (Lower Cretaceous) Khok Kruat Formation, the stratigraphically youngest fossil-bearing Mesozoic Thai stratigraphic unit. Based on a partial postcranial skeleton, we present the first diagnostic sauropod specimen from this formation, which represents a new somphospondylan titanosauriform, *Nagatitan chaiyaphumensis* n. gen. n. sp. *Nagatitan* is diagnosed by two autapomorphies and a unique character combination, including the presence of two distinct hyposphene-hypantrum morphologies within the middle–posterior dorsal vertebrae. Phylogenetic analyses under maximum parsimony, using a data matrix containing 153 taxa and 570 characters, produce well-resolved topologies that place *Nagatitan* within the somphospondylan clade Euhelopodidae. *Nagatitan* does not form an endemic subclade with the approximately contemporaneous Southeast Asian euhelopodids *Phuwiangosaurus* and *Tangvayosaurus*, with a suite of anatomical features distinguishing these taxa. We estimate a body mass of 25–28 tonnes for *Nagatitan*, and suggest it was part of a broader middle Cretaceous body size increase in Asian titanosauriforms, facilitated by rising temperatures and expanded suitable habitat. The discovery of *Nagatitan* expands the known diversity of Southeast Asian sauropods and improves our understanding of titanosauriform biogeography within the region.

Somphospondylan titanosauriforms were a diverse and globally distributed clade of sauropod dinosaurs that appeared in the Late Jurassic or earliest Cretaceous and persisted through to the Cretaceous/Paleogene boundary[1–3]. A substantial proportion of this diversity comes from the Cretaceous of Asia (e.g.,[4–6]) and includes a number of species thought to belong to the endemic somphospondylan clade Euhelopodidae. The monophyly, phylogenetic position, and composition of Euhelopodidae has been extensively debated (e.g.,[2,4,7,8]), with some earlier studies supporting a placement outside of Neosauropoda[9,10,10,11,11]. However, most analyses now agree that Euhelopodidae represents an early-diverging somphospondylan clade. To date, two valid euhelopodid species have been recognised from Southeast Asia: *Phuwiangosaurus sirindhornae*, from the upper Valanginian–Barremian (Lower Cretaceous) Sao Khua Formation of Thailand[12,13], and *Tangvayosaurus hoffeti*, from the Aptian–Albian (Lower Cretaceous) Grés supérieurs Formation of Laos[14]. In phylogenetic analyses wherein both of these species are included, they are typically recovered as sister taxa (e.g.,[2,15]), which might imply that they represent a locally endemic euhelopodid subclade. Nevertheless, their interrelationships with other euhelopodid taxa tend to be unstable. This lack of consensus is likely due to several factors, including missing data resulting from incomplete preservation and/or a lack of detailed anatomical information reported in descriptive studies.

[1]Department of Earth Sciences, University College London, London WC1E 6BT, UK. [2]Department of Mineral Resources, Sirindhorn Museum, Sahatsakhan 46140, Kalasin, Thailand. [3]Palaeontological Research and Education Centre, Mahasarakham University, Khamriang 44150, Maha Sarakham, Thailand. [4]Excellence Centre in Evolution of Life, Basin Studies and Applied Palaeontology, Mahasarakham University, Khamriang 44150, Maha Sarakham, Thailand. [5]Institute of Engineering, School of Geotechnology, Suranaree University of Technology, 111 University Avenue, Muang 30000, Nakhon Ratchasima, Thailand. [6]Thitiwoot Sethapanichsakul and Sasa-On Khansubha have contributed equally to this work. ✉email: sita.m@msu.ac.th

Thus, the discovery and description of new specimens and revision of existing ones are essential to test the competing hypotheses regarding the interrelationships of Asian Cretaceous somphospondylans.

The Aptian–Albian Khok Kruat Formation, the stratigraphically youngest fossil-bearing Mesozoic unit in Thailand, is notable for its diverse vertebrate assemblage, which includes fish, sharks, turtles, crocodyliforms, pterosaurs, ornithischians, and theropods[16–19]. The vertebrate fauna of the Khok Kruat Formation shows similarities to that of the Aptian Xinlong Formation of China[17] and the aforementioned Grès supérieurs Formation of Laos[20–22]. Both of these formations have yielded sauropods, with named taxa from the Xinlong Formation comprising the titanosauriforms *Fusuisaurus zhaoi* and *Liubangosaurus hei*, alongside *Tangvayosaurus* from the Grès supérieurs Formation[14,23,24]. Previous sauropod discoveries from the Khok Kruat Formation have been limited to isolated teeth and fragmentary postcranial remains of uncertain taxonomic affinities[18,19,25].

Here we describe the partial skeleton of a new sauropod taxon from the Khok Kruat Formation that outcrops at the Ban Pha Nang Sua locality, northeastern Thailand. We incorporate this taxon into a recent phylogenetic data matrix and analyse its relationships with other sauropods under maximum parsimony, using both equal and extended implied weighting. Finally, we compare the new taxon with other contemporaneous Southeast and East Asian sauropods and consider the implications of its phylogenetic relationships for our wider understanding of the evolution of the group.

Geological and taphonomic setting

The Khok Kruat Formation is the stratigraphically uppermost Mesozoic-aged sedimentary unit in the Khorat Group of northeastern Thailand[26,27]. Palynomorph data indicate an upper Aptian age, with the possibility that the upper part of the formation extends into the Albian based on the overlying Albian–Cenomanian Mahasarakham Formation[22]. The shared occurrence of the freshwater shark *Thaiodus ruchae* in the Khok Kruat Formation and the Takena Formation of the Lhasa block of Tibet[28], which is dated as Aptian–Albian on the basis of Foraminifera[19,20], further supports a late Early Cretaceous age. A rich record of invertebrates and vertebrates has been documented from the Khok Kruat Formation, revealing a diverse faunal assemblage that includes: bivalves, various actinopterygian fish[29–31], numerous hybodont sharks[32–35], freshwater turtles[16,36], a neosuchian crocodylomorph[37], a goniopholidid crocodyliform[18],an atoposaurid crocodyliform[38], an anurognathid pterosaur[39,40], an azhdarchoid pterosaur[39,40], an ornithocheiriform pterosaur[18,39], non-hadrosaurid iguanodontians[18,19,41–43], early-branching ceratopsians[18–20], an ornithomimosaurian[44], a carcharodontosaurian[17], and a spinosaurid[18,19]. Indeterminate sauropod remains have also been discovered from the Khok Kruat Formation[18,19]. Sekiya et al.[25] noted the discovery of two peg-like tooth morphologies, an incomplete middle cervical vertebra with similarities to *Phuwiangosaurus*, and an incomplete proximal end of a dorsal rib. They tentatively identified the specimens as originating from a titanosauriform similar to *Euhelopus* but no further identification could be performed due to the fragmentary preservation and lack of diagnostic features in the material[25].

The Ban Pha Nang Sua locality is situated in the Nong Bua Rawe District of Chaiyaphum Province, northeastern Thailand[18] (Fig. 1). Fossils were initially discovered by a local resident in 2016 during the dry season, when lower water levels had exposed the bone bed on the side of a communal pond. Initial fieldwork was carried out from 2016 to 2019, during which several skeletal elements were discovered, excavated, and subsequently moved to the Sirindhorn Museum for preparation. Excavation of the remaining specimens began in early 2024 and was completed that same year. The geological composition of the locality primarily consists of the Khok Kruat Formation and overlying Quaternary sediments[45,46]. The stratigraphic sequence at the locality is well-preserved at the edge of the pond and depicts a depositional environment defined by cycles of sedimentation resulting from a meandering river system in a semi-arid paleoenvironment. Approximately 3.96 m thick, the sequence can be delineated into nine distinct lithologic units (units 1–9, from bottom to top) (Fig. 2) based on their lithologies and faunal assemblages. The sauropod individual described herein originates from unit 1, with indeterminate bivalves, allosauroid and spinosaurid teeth, and teeth from the freshwater shark *Heteroptychodus steinmanni* all from unit 3[18]. Both units are composed of reddish-brown calcareous siltstones displaying climbing ripple cross-lamination, with a thickness of approximately 1.50 and 0.53 m, respectively.

The full inventory of sauropod specimens excavated from unit 1 comprises: four dorsal vertebrae, four sacral vertebrae, five dorsal ribs, right humerus, right ilium, left and right pubis, a mostly complete right femur, and indeterminate fragments (Fig. 3). Based on the lack of duplicated elements, their consistency in size, and their close association, the sauropod remains are inferred to belong to a single individual. All specimens have been stored and accessioned within the Sirindhorn Museum (SM) in Kalasin Province.

Results

Systematic palaeontology

Dinosauria Owen, 1842
Saurischia Seeley, 1887
Sauropoda Marsh, 1878
Titanosauriformes Salgado, Coria & Calvo, 1997
Somphospondyli Wilson & Sereno, 1998
Euhelopodidae Romer, 1956 (sensu D'Emic, 2012)
Nagatitan chaiyaphumensis gen. et sp. nov.

Etymology: The generic name is derived from *Naga*, referring to the mythological serpent-like creature found in various Asian cultures, especially in northeastern Thailand, often associated with water and Buddhism, and *titan*, a giant in Greek mythology. The specific epithet is derived from the province of Chaiyaphum, Thailand.

Holotype: SM2025-1-546 to SM2025-1-556—four dorsal vertebrae, five dorsal ribs, four sacral vertebrae, five sacral ribs, right humerus, right ilium, left and right pubis, mostly complete right femur.

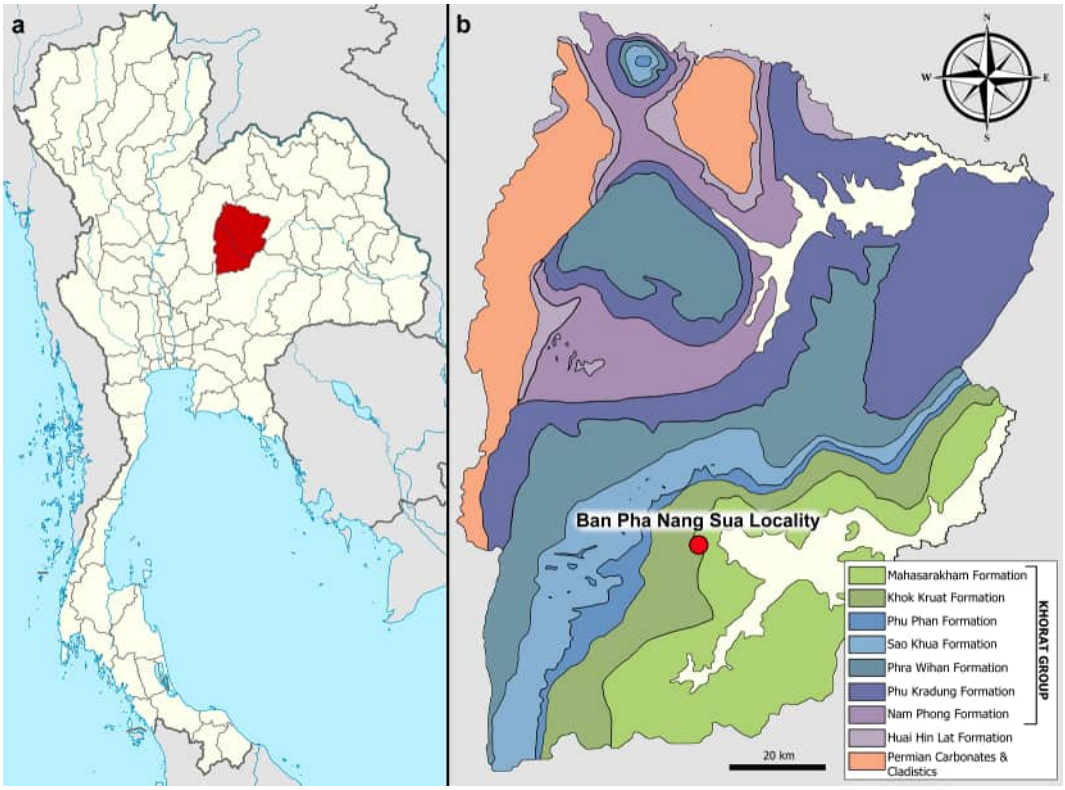

Fig. 1. Geographic position of (**a**) Chaiyaphum Province on a map of Thailand[122] and (**b**) Ban Pha Nang Sua locality on a geological map of Chaiyaphum Province. This map was drafted by the first author T.S, modified from the geological map of northeastern Thailand created by Hongsabal (2023)[123] for the Department of Mineral Resources, Thailand. Scale bar is 20 km.

Diagnosis: Nagatitan can be diagnosed by a unique combination of characters (autapomorphies denoted with an asterisk): (1) paired postzygapophyseal centrodiapophyseal fossa present on posterior dorsal neural arches; (2*) hyposphene of middle dorsal vertebrae exhibits a triangular morphology, becoming a vertical ridge in posterior dorsal vertebrae; (3) parapophysis positioned dorsal to the prezygapophysis on posterior dorsal neural arches; (4) spinopostzygapophyseal laminae of middle and posterior dorsal neural spines divided into lateral and medial branches throughout their length; (5) bifurcated middle dorsal neural spines; (6*) triangular anterior aliform processes present on posterior dorsal neural spines; (7) prominent bulge on posterolateral margin of humerus, approximately level with the deltopectoral crest, that interrupts the lateral humeral margin in anterior view; (8) rounded proximolateral corner of humerus; (9) humeral shaft exhibits a high eccentricity value (>2.5); (10) distal end of the pubis transversely expanded along the lateral surface relative to the shaft; and (11) proximal third of femur with anteroposteriorly narrowed lateral margin forming a flange-like trochanteric shelf and a medially bounding vertical ridge along the posterior surface.

Locality and Horizon: Ban Pha Nang Sua, Nong Bua Rawe District, Chaiyaphum Province, Thailand; Khok Kruat Formation, Aptian–Albian, upper Lower Cretaceous (Fig. 4).

Description and comparisons

Dorsal vertebrae

Four dorsal vertebrae are preserved (Table 1), all of which represent middle to posterior dorsal vertebrae based on the position of the parapophysis on the neural arch. SM2025-1-546 (Fig. 5) is a middle dorsal vertebra that is relatively complete, with only slight lateral distortion. It lacks the left parapophysis and part of the left diapophysis. SM2025-1-547 (Fig. 6) is a near-complete posterior dorsal vertebra, with only the left transverse process missing. It is slightly distorted, with the posterior end of the centrum being skewed ventrolaterally with respect to the anterior end. SM2025-1-548 (Fig. 7) is an incomplete posterior dorsal vertebra that lacks its transverse processes. Taphonomic lateral compression has elongated the specimen anteroposteriorly. SM2025-1-549 (Fig. 7) is the least complete and most deformed of the four dorsal vertebrae. It preserves the centrum and most of the neural arch, but lacks most of the neural spine and transverse processes. It is severely crushed laterally and broken into two pieces. This poor preservation makes it difficult to determine its position beyond an identification as a middle–posterior dorsal vertebra.

All four dorsal centra are anteroposteriorly short and opisthocoelous. The anterior condyle is prominent in SM2025-1-547, SM2025-1-548 and SM2025-1-549, whereas it appears reduced in SM2025-1-546. However, the latter is incompletely preserved in this region. The damaged anterior condyle of SM2025-1-546 reveals that the internal tissue structure of the centrum is camellate, as is the case in other titanosauriforms[47]. Both the

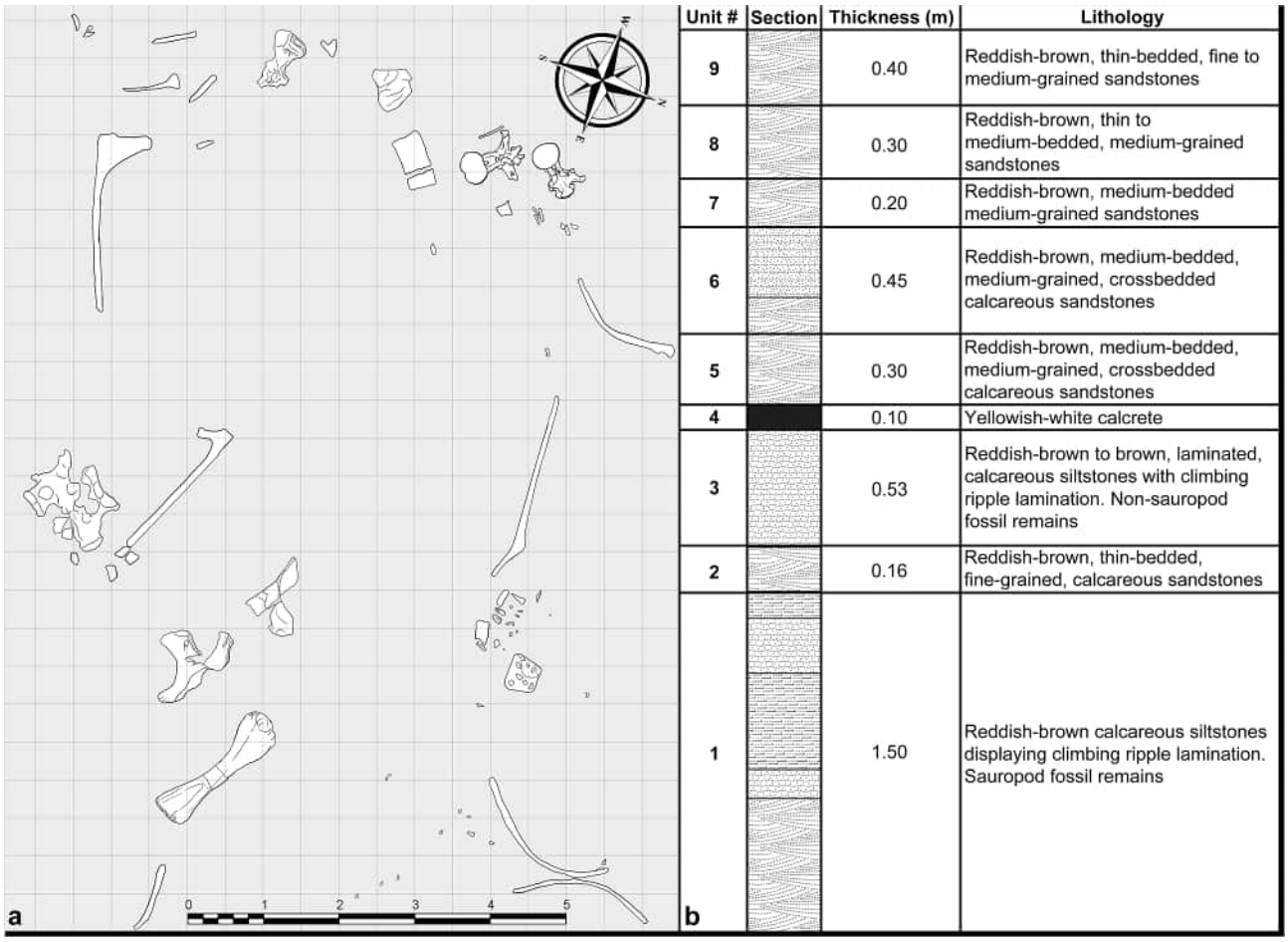

Unit #	Section	Thickness (m)	Lithology
9		0.40	Reddish-brown, thin-bedded, fine to medium-grained sandstones
8		0.30	Reddish-brown, thin to medium-bedded, medium-grained sandstones
7		0.20	Reddish-brown, medium-bedded medium-grained sandstones
6		0.45	Reddish-brown, medium-bedded, medium-grained, crossbedded calcareous sandstones
5		0.30	Reddish-brown, medium-bedded, medium-grained, crossbedded calcareous sandstones
4		0.10	Yellowish-white calcrete
3		0.53	Reddish-brown to brown, laminated, calcareous siltstones with climbing ripple lamination. Non-sauropod fossil remains
2		0.16	Reddish-brown, thin-bedded, fine-grained, calcareous sandstones
1		1.50	Reddish-brown calcareous siltstones displaying climbing ripple lamination. Sauropod fossil remains

Fig. 2. (**a**) Bone map and (**b**) stratigraphic column of the Ban Pha Nang Sua locality. Scale bar is 5 m. Thickness given in meters.

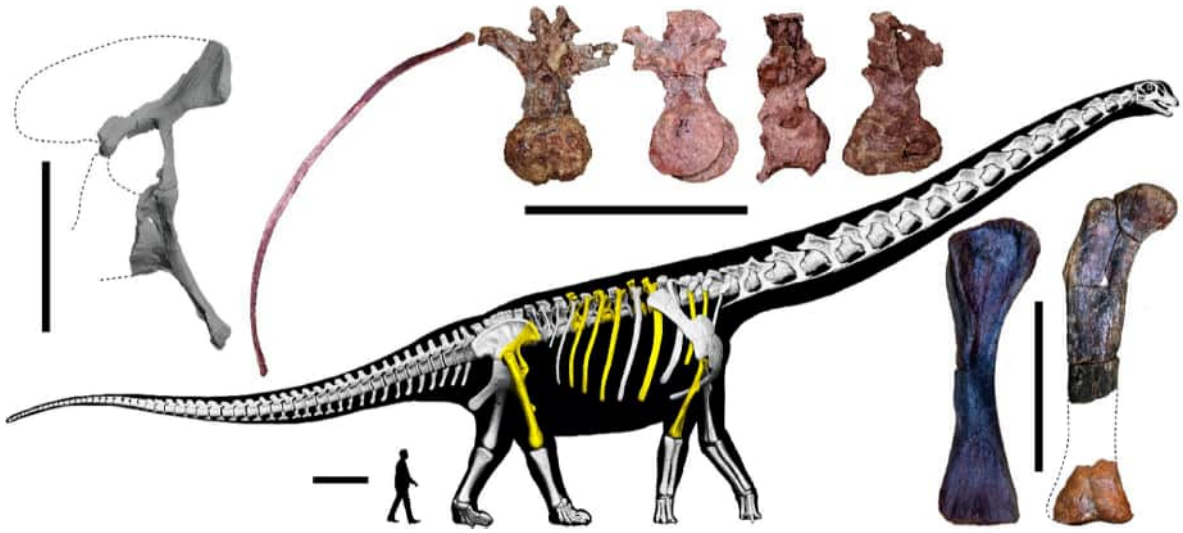

Fig. 3. Schematic representation of the skeleton of *Nagatitan chaiyaphumensis* gen. et sp. nov. Preserved bones are highlighted. Scale bar equals 1 m.

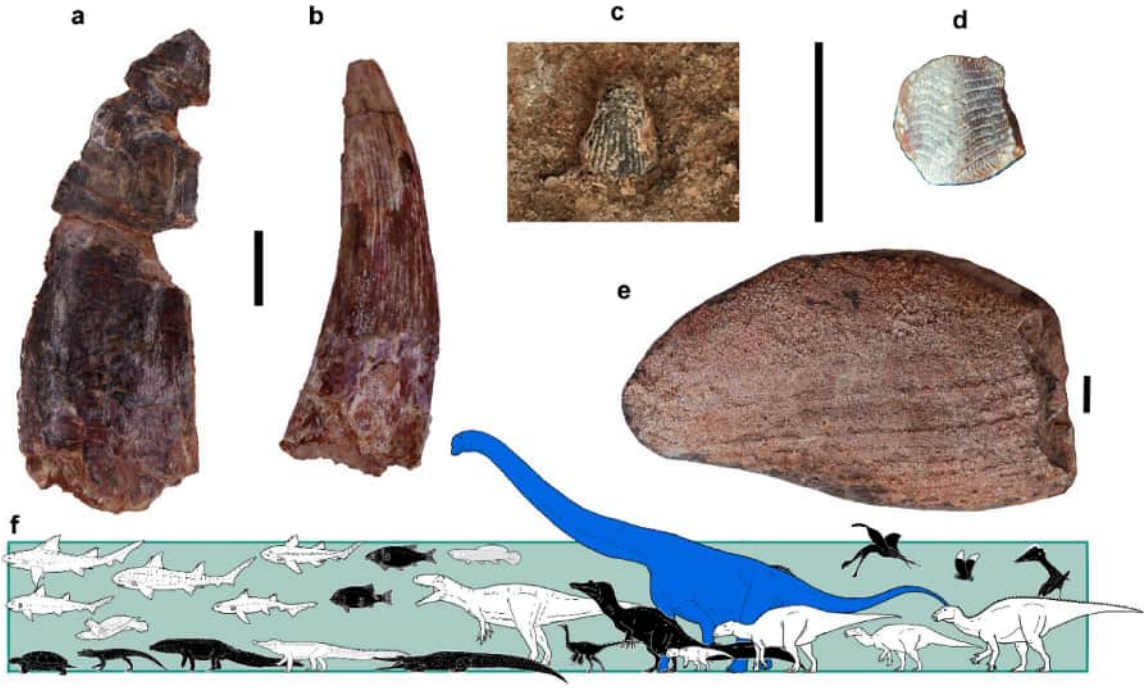

Fig. 4. Non-sauropod faunal remains discovered in the Ban Pha Nang Sua locality: (**a**) Allosauroid tooth (SDM2025-1-562) in labial view, (**b**) spinosaurid tooth (SDM2025-1-561) in labial view, (**c**) crocodyliform tooth (specimen lost during the excavation) in lingual view, (**d**) *Heteroptychodus steinmanni* tooth (SDM2025-1-563) in apical view, and (**e**) mold of cf. *Yunnanoconcha* sp. (SDM2025-1-560) in external view. (**f**) Stylized illustration displaying the vertebrate fauna assemblage known from the Khok Kruat Formation modified from Manitkoon et al. 2023[18]. Shaded black silhouette indicate tentative taxa. *Nagatitan chaiyaphumensis* gen. et sp. nov. shaded in blue. Scale bars equal 10 mm.

	CL	CL+	ACH	ACW	PCH	PCW	NAH	NSH	NSL	NSW	PRL	PRW	PRFH	PRFW	POL	POW	POFH	POFW
SM2025-1-546	150	245	253	361	250	350	235	278	123	180	195	172	55	113	196	200	51	123
SM2025-1-547	154	221	276	330	308	363	180	286	110	280	113	294	30	125	116	315	63	138
SM2025-1-548	210*	–	226*	–	260*	–	250*	224*	90*	141*	108*	143*	57*	57*	79*	180*	54*	82*
SM2025-1-549	230*	–	273*	–	330*	–	213*	–	–	–	–	–	–	–	–	–	–	–

Table 1. Measurements of dorsal vertebrae of *Nagatitan chaiyaphumensis* gen. et. sp. nov. CL, centrum length excluding condyle; CL+, Centrum length including condyle; ACH, anterior condyle dorsoventral height; ACW, anterior condyle mediolateral width; PCH, posterior cotyle dorsoventral height; PCW, posterior cotyle mediolateral width; NAH, neural arch dorsoventral height; NSH, neural spine dorsoventral height; NSL, neural spine base anteroposterior length; NSW, neural spine base mediolateral width; PRL, prezygapophysis anteroposterior length; PRW, prezygapophysis mediolateral breadth; PRFH, prezygapophyseal articular facet height; PRFW, prezygapophyseal articular facet width; POL, postzygapophyseal length; POW, postzygapophyseal width; POFH, postzygapophyseal articular facet anteroposterior width; POFW, postzygapophyseal articular facet mediolateral width. *Indicates uncertain values due to incomplete or deformed specimen. Measurements are in mm.

anterior and posterior articular surfaces of the centra are subcircular, being slightly wider transversely than dorsoventrally tall (Table 1). In SM2025-1-546, the posterior articular surface has a mediolateral width to dorsoventral height ratio that is greater than 1.4. The posterior cotyle is concave in all four dorsal centra, being deepest in SM2025-1-547.

Overall, the ventral surface of each centrum is mostly flat, although it becomes transversely convex along the midline, forming a low, rounded ridge in SM2025-1-547, and a more prominent ridge in SM2025-1-548. This resembles the ventral keel seen in some brachiosaurids[7], and that is also variably present in the middle–posterior dorsal centra of *Phuwiangosaurus*[48,49] and some titanosaurs[50]. In lateral view, the ventral margin of the centrum is strongly arched upwards, with this especially prominent in SM2025-1-546 and SM2025-1-547. The lateral pneumatic foramina are restricted to the dorsal third of the lateral surface of the centrum, situated closer to the anterior than posterior margin of the non-condylar centrum. As is the case in many somphospondylans[7], the

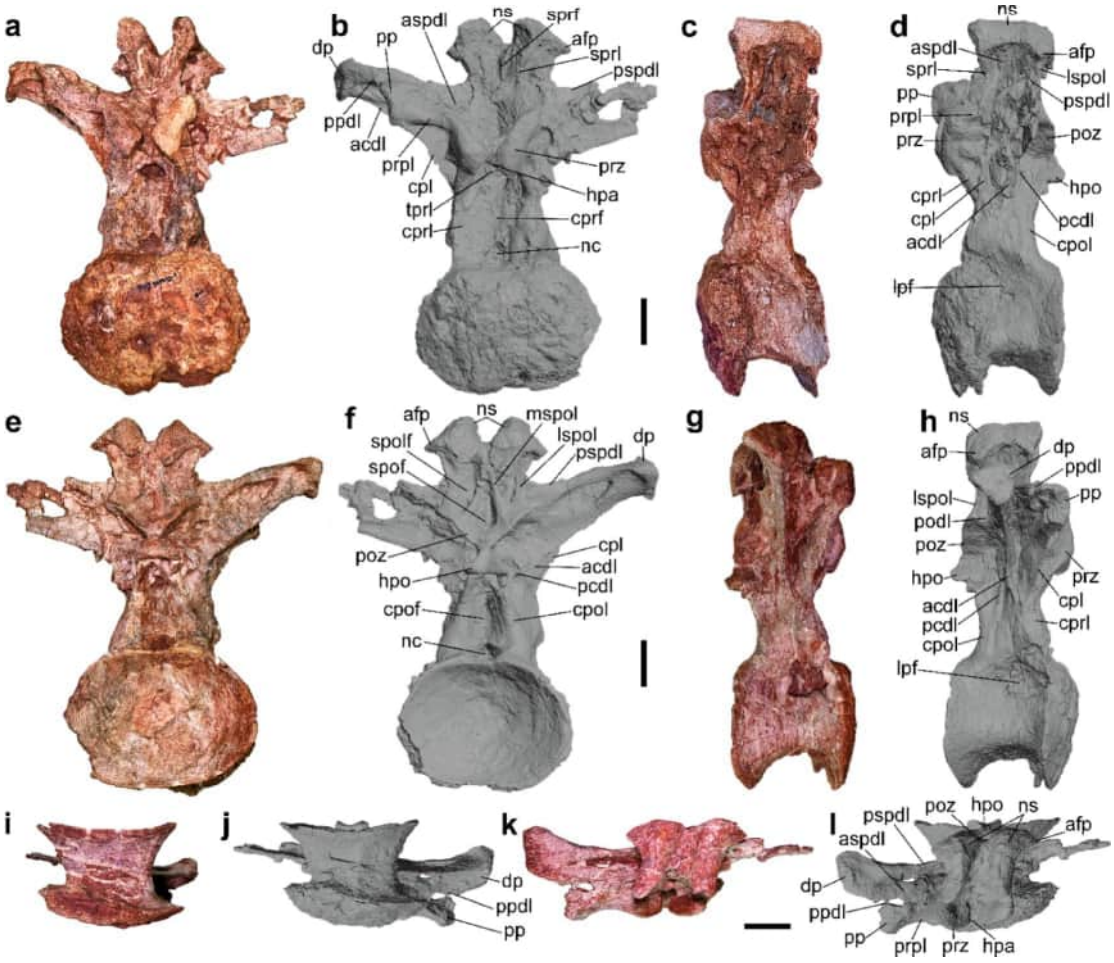

Fig. 5. Photographs and 3D surface scan model images of the middle dorsal vertebra (SM2025-1-546) of *Nagatitan chaiyaphumensis* gen. et sp. nov. in (**a**, **b**) anterior, (**c**, **d**) left lateral, (**e**, **f**) posterior, (**g**, **h**) right lateral, (**i**, **j**) ventral and (**k**, **l**) dorsal views. Scale bars equal 100 mm. a.afp, anterior aliform process; a.spdl, anterior spinodiapophyseal lamina; acdl, anterior centrodiapophyseal lamina; acpl, anterior centroparapophyseal lamina; cpof, centropostzygapophyseal fossa; cprf, centroprezygapophyseal fossa; dp, diapophysis; hpa, hypantrum; hpo, hyposphene; lpf, lateral pneumatic fossa; p.afp, posterior aliform process; p.spdl, posterior spinodiapophyseal lamina; pcdl, anterior centrodiapophyseal lamina; podl, postzygodiapophyseal lamina; poz, postzygapophysis; pp, parapophysis; ppdl, paradiapophyseal lamina; prdl, prezygodiapophyseal lamina; prpl, prezygoparapophyseal lamina; prz, prezygapophysis; spof, spinopostzygapophyseal fossa; spol, spinopostzygapophyseal lamina; sprl, spinoprezygapophyseal lamina; tprl, interprezygapophyseal lamina.

foramina are set within a lateral fossa. The foramina are deep excavations that are dorsoventrally short and oval in outline, with a sub-acute posterior margin.

In SM2025-1-546, the anterior opening of the neural canal is subcircular, with an acute dorsal margin, whereas that of SM2025-1-547 is rhomboidal. The posterior neural canal opening of both specimens is oval, with dorsal margins that narrow to an acute dorsal tip. The anterior neural canal opening is enclosed in a deep centroprezygapophyseal fossa (CPRF), contrasting with the condition in many titanosaurs[50,51]. Robust, vertically oriented centroprezygapophyseal laminae (CPRLs) form the lateral margins of the CPRF. In SM2025-1-547, the CPRF is divided into two shallow depressions on the anterior surface of the neural arch, bounded by the CPRLs, located just ventral to each prezygapophysis. These fossae are formed by the accentuated dorsal edge of the neural canal, the medial margins of the CPRLs, and the V-shaped interprezygapophyseal lamina (TPRL). The ventral tip of the TPRL contacts the dorsal margin of the neural canal, forming an X-shaped lamina complex on the anterior face of the neural arch. This morphology is similar to that observed in the middle–posterior dorsal vertebrae of the probable euhelopodid *Yongjinglong*[15,52], as well as several titanosaurs, e.g. *Lirainosaurus*[53] and *Tapuiasaurus*[54]. A deep triangular fossa that is approximately as transversely wide as the anterior opening of the neural canal is formed by the dorsal margin of the V-shaped TPRL and the ventral margin of the prezygapophysis. SM2025-1-546 also appears to exhibit the V-shaped TPRL morphology; however, the ventral margin of the TPRL does not contact the dorsal margin of the neural canal to form the X-shaped complex observed in SM2025-1-547. A deep subtriangular fossa is located just ventral to the TPRL in SM2025-1-546. A similar fossa is also located on the posterior face of the specimen's neural arch, just below the hyposphene. SM2025-1-547 exhibits a

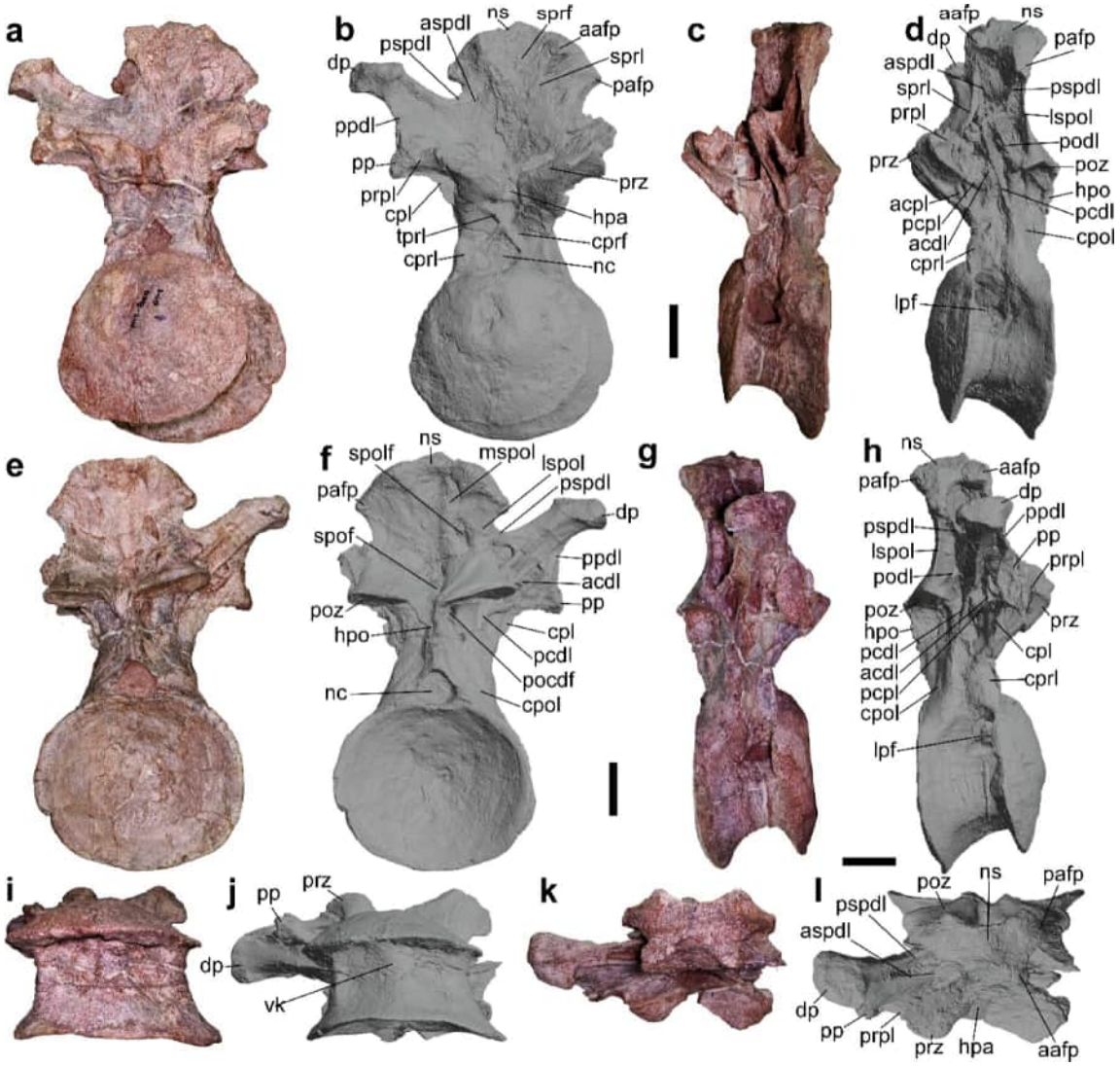

Fig. 6. Photographs and 3D surface scan model images of the posterior dorsal vertebra (SM2025-1-547) of *Nagatitan chaiyaphumensis* gen. et sp. nov. in (**a**, **b**) anterior, (**c**, **d**) left lateral, (**e**, **f**) posterior, (**g**, **h**) right lateral, (**i**, **j**) ventral and (**k**, **l**) dorsal views. Scale bars equal 100 mm. a.afp, anterior aliform process; a.spdl, anterior spinodiapophyseal lamina; acdl, anterior centrodiapophyseal lamina; acpl, anterior centroparapophyseal lamina; cpof, centropostzygapophyseal fossa; cprf, centroprezygapophyseal fossa; dp, diapophysis; hpa, hypantrum; hpo, hyposphene; lpf, lateral pneumatic fossa; p.afp, posterior aliform process; p.spdl, posterior spinodiapophyseal lamina; pcdl, anterior centrodiapophyseal lamina; podl, postzygodiapophyseal lamina; poz, postzygapophysis; pp, parapophysis; ppdl, paradiapophyseal lamina; prdl, prezygodiapophyseal lamina; prpl, prezygoparapophyseal lamina; prz, prezygapophysis; spof, spinopostzygapophyseal fossa; spol, spinopostzygapophyseal lamina; sprl, spinoprezygapophyseal lamina; tprl, interprezygapophyseal lamina.

similar fossa located on the anterior face of the neural arch, dorsal to the TPRL, but does not possess a fossa on the posterior face such as that seen on SM2025-1-546.

The prezygapophyses are large and directed anterodorsally. Their anterior margins extend slightly beyond the anterior margin of the condyle in SM2025-1-547 and SM2025-1-548 but do not do so in SM2025-1-546. The articular facet of each prezygapophysis is flat with an outline that has rounded margins. The angle of the prezygapophyseal articular facets varies throughout the series. In particular, the articular surfaces of the prezygapophyses in the middle dorsal vertebra (SM2025-1-546) are angled at approximately 45° with respect to the horizontal, such that they face dorsomedially. In the posterior dorsal vertebra (SM2025-1-547), the prezygapophyses are angled at approximately 25° to the horizontal. Each dorsal vertebra has postzygapophyseal articulation angles corresponding to those of its prezygapophyses. A strongly dorsomedially oriented middle dorsal zygapophyseal articulation angle greater than 40° is almost exclusively found in titanosaurs[50,51], with *Daxiatitan*[55] and *Ruyangosaurus*[56,57] being the only non-titanosaurian somphospondylans exhibiting a similar morphology. A low angle in posterior neural arches is common in most sauropods, contrasting with the steeply

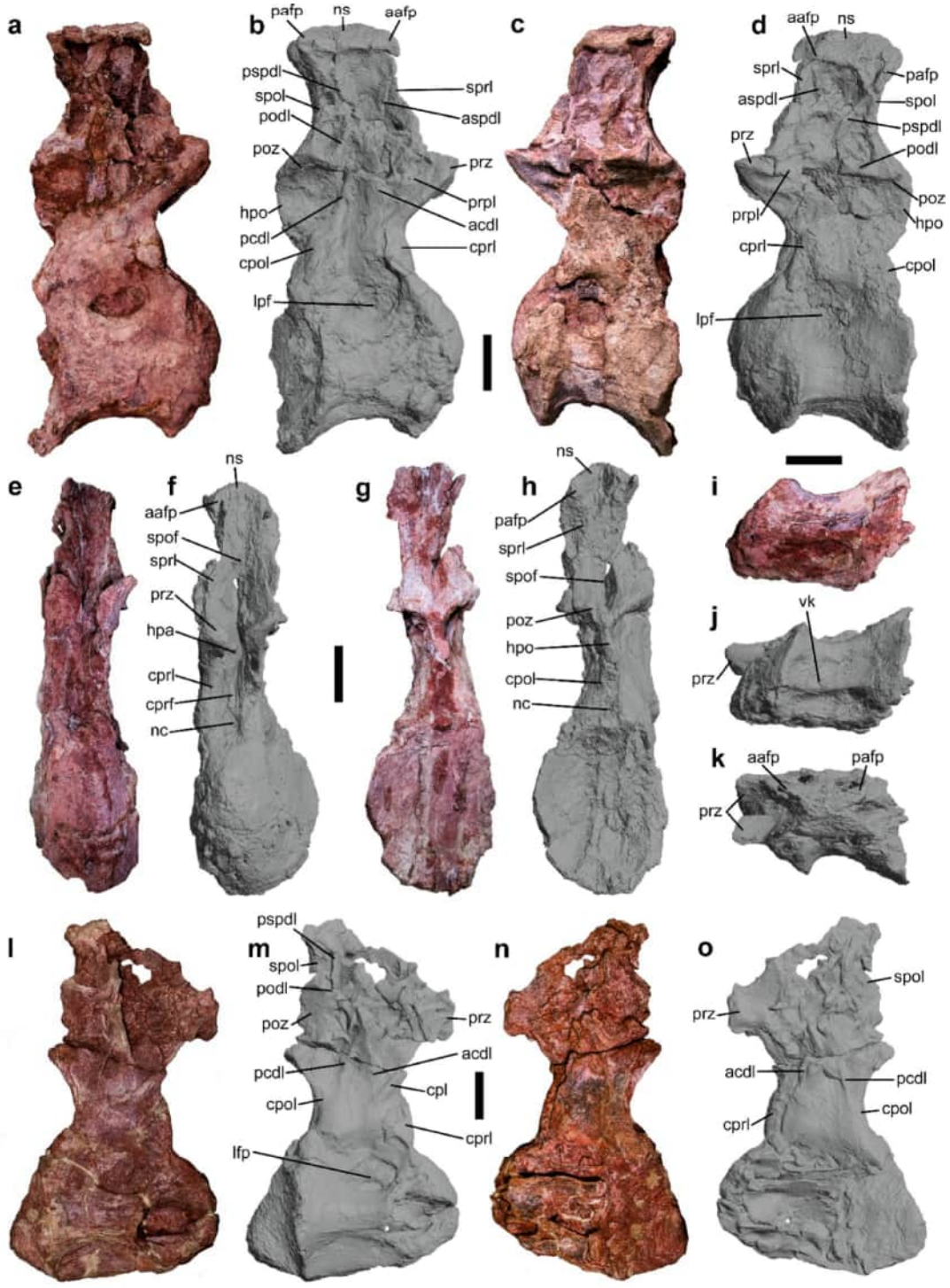

Fig. 7. Photographs and 3D surface scan model images of the posterior dorsal vertebra (SM2025-1-548) (**a**–**k**) and incomplete dorsal vertebra (SM2025-1-549) (**l**–**o**) of *Nagatitan chaiyaphumensis* gen. et sp. nov. in (**a**, **b**, **l**, **m**) right lateral, (**c**, **d**, **n**, **o**) left lateral, (**e**, **f**) anterior, (**g**, **h**) posterior, (**i**, **j**) ventral and (**k**) dorsal views. Scale bars equal 100 mm. a.afp, anterior aliform process; a.spdl, anterior spinodiapophyseal lamina; acdl, anterior centrodiapophyseal lamina; acpl, anterior centroparapophyseal lamina; cpof, centropostzygapophyseal fossa; cprf, centroprezygapophyseal fossa; dp, diapophysis; hpa, hypantrum; hpo, hyposphene; lpf, lateral pneumatic fossa; p.afp, posterior aliform process; p.spdl, posterior spinodiapophyseal lamina; pcdl, posterior centrodiapophyseal lamina; podl, postzygodiapophyseal lamina; poz, postzygapophysis; pp, parapophysis; ppdl, paradiapophyseal lamina; prdl, prezygodiapophyseal lamina; prpl, prezygoparapophyseal lamina; prz, prezygapophysis; spof, spinopostzygapophyseal fossa; spol, spinopostzygapophyseal lamina; sprl, spinoprezygapophyseal lamina; tprl, interprezygapophyseal lamina.

inclined zygapophyses of many titanosaurs[50,51]. The postzygapophyses have oval and slightly concave articular surfaces.

A hypantrum-hyposphene complex is preserved in SM2025-1-546, SM2025-1-547, and SM2025-1-548. *Nagatitan* exhibits two different hyposphene morphologies. The middle dorsal vertebra, SM2025-1-546, possesses a triangular hyposphene. It extends anteroposteriorly beyond the posterior surface of the postzygapophyses and is mediolaterally wider than it is dorsoventrally tall. The hyposphene becomes a vertical ridge in the posterior dorsal vertebrae. We interpret this ridge as a reduced hyposphene, rather than a singular interpostzygapophyseal lamina (sTPOL), given that its posterior surface is level with or extends further posteriorly than the posterior surface of the postzygapophyses in both SM2025-1-547 and SM2025-1-548; by contrast, a sTPOL is typically anteriorly offset from the posterior surface of the postzygapophyses (e.g.,[49,58]). This interpretation is supported by the hyposphene in SM2025-1-547, which, although not completely preserved, appears to exhibit a transitional morphology between the triangular and vertical ridge shape. The posterior surface of the hyposphene of SM2025-1-547 also exhibits a concavity that runs vertically along the midline, extending from its dorsal margin to where the hyposphene tapers to a vertical ridge that contacts the dorsal margin of the neural canal. The hyposphene of SM2025-1-548 forms a transversely thick vertical ridge. Variation of hyposphene morphology within the dorsal series has been occasionally observed in other sauropods, such as in *Omeisaurus*[59]. In all cases, this variation is represented by a slight modification of the hyposphene morphology, but the overall shape is maintained, or the hyposphene is lost in the posterior dorsal vertebrae[60]. As such, we regard this combination of triangular and vertical ridge hyposphene morphologies as an autapomorphy of *Nagatitan*.

The parapophysis of SM2025-1-546 is situated dorsal and posterolateral to the prezygapophyses, with the articular surface of the parapophysis located just below the level of that of the diapophysis. In SM2025-1-547, the parapophysis remains dorsal and posterolateral to the prezygapophyses, but it is positioned lower dorsoventrally than in SM2025-1-546. A parapophysis positioned dorsal to the prezygapophysis on the posterior dorsal neural arches is only otherwise present in turiasaurians and rebbachisaurids[3,61]. The subhorizontal prezygoparapophyseal (PRPL) and paradiapophyseal lamina (PPDL) are both anteroposteriorly short. The anterior centroparapophyseal lamina (ACPL) extends ventrally and slightly anterior to the base of the CPRL. The posterior centroparapophyseal lamina (PCPL) is undivided, highly reduced, and is oriented anterodorsally-to-posteroventrally in both SM2025-1-546 and SM2025-1-547. Undivided PCPLs have been observed in many somphospondylans[2,7]. In posterolateral view, the near-vertical anterior centrodiapophyseal lamina (ACDL) is only preserved in SM2025-1-547. The ACDL runs parallel to the ACPL, but extends past the parapophysis and contacts the anterior margin of the diapophysis where it meets the main body of the neural arch. The posterior centrodiapophyseal lamina (PCDL) remains thin and unexpanded at its ventral tip, where it merges with the centropostzygapophyseal lamina (CPOL), similar to the condition in *Phuwiangosaurus*[12,13]. Several titanosauriforms possess an apomorphic condition in which the ventral end of the PCDL is expanded or bifurcated[1], but in *Nagatitan* the PCDL retains the plesiomorphic unexpanded condition. An unexpanded ventral PCDL also characterises several other somphospondylans[7], including *Chubutisaurus*[62], *Dongbeititan*[63], *Europatitan*[64], *Phuwiangosaurus*[12,13], and *Tastavinsaurus*[65].

The CPOL is divided into lateral and medial branches that narrow transversely as they extend dorsomedially from the centrum. The medial branches of the CPOL meet the ventrolateral corners of the hyposphene. A centropostzygapophyseal fossa (CPOF) is observable in SM2025-1-546 and SM2025-1-548. The CPOF of SM2025-1-546 is dorsoventrally tall and narrows mediolaterally towards its dorsal end. In SM2025-1-547, the CPOF is absent, but there are paired postzygapophyseal centrodiapophyseal fossae (POCDF) located ventromedial to the postzygapophyseal articular surfaces, where the latter meet the hyposphene. The POCDFs are small, circular, and ramify deeply into the neural arch. SM2025-1-548 potentially possesses a similar POCDF to SM2025-1-547, but the specimen is too incomplete in this region, whereas SM2025-1-546 exhibits a shallow POCDF. The POCDF of SM2025-1-547 is bordered by the CPOL, postzygapophyses, and the hyposphene. POCDFs are typically more shallow and located in a more lateral position in other sauropods, with this feature bordered by the CPOL, postzygodiapophyseal lamina (PODL) and PCDL; this includes rebbachisaurines[66], *Yongjinglong*[52], and a few titanosaurs, such as *Igai*[67], *Dreadnaughtus*[68], and *Tapuisaurus*[54]. The POCDF of *Nagatitan* most closely resembles that of the posteriormost dorsal vertebrae of *Haplocanthosaurus*[69] in their shape and position.

The diapophyses are short and dorsoventrally taller than anteroposteriorly wide, differing from the elongate processes of brachiosaurids[2]. The PODL is short and extends anterodorsally-to-posteroventrally in SM2025-1-546 to 548. The distal extent of each diapophysis is slightly offset from the remaining dorsal surface of the process by a lip. This is most developed in SM2025-1-547 and less so in SM2025-1-546. This distinct dorsal surface characterises many somphospondylans[2], including *Phuwiangosaurus*[12,13]. In SM2025-1-546, the diapophyses project approximately 30 degrees dorsolaterally above the horizontal plane, whereas in SM2025-1-547 the angle of projection is closer to 45 degrees.

The neural spines are dorsoventrally short, robust, and rectangular in lateral view. The dorsal apex of the neural spine is also transversely broad in *Nagatitan*, unlike the mediolaterally tapering and acute neural spine summits seen in *Phuwiangosaurus*[12,13]. SM2025-1-548 differs from the other three specimens in that its neural spine is angled slightly posteriorly, although this is probably the result of taphonomic distortion. The ratio of dorsoventral height of the posterior dorsal neural spine to posterior centrum articular face height is 0.93 in SM2025-1-547. A posterior dorsal spine to centrum height ratio below 1.0 is similar to that of most Asian somphospondylans, including *Phuwiangosaurus*[7,15]. The neural spine of SM2025-1-547 exhibits a transversely expanded 'fan'-shaped morphology, similar to that observed in the middle–posterior dorsal vertebrae of some early-diverging macronarians, including *Camarasaurus*[70], *Giraffatitan*[71], and Yuzhoulong[72]. SM2025-1-546 has a bifurcated neural spine, whereas the neural spines of SM2025-1-547 and SM2025-1-548 are non-bifid, suggesting that bifurcation did not continue into the posterior dorsal vertebrae. Bifurcated middle dorsal neural spines characterise a number of flagellicaudatans and somphospondylans, including *Daxiatitan*[55], *Dongyangosaurus*[73],

and *Liubangosaurus*[23], as well as some titanosaurs[7]. Although the cervical and anterior dorsal neural spines are bifid in *Euhelopus*[4] and *Phuwiangosaurus*[12,13], this does not extend into the middle dorsal vertebrae.

The spinoprezygapophyseal lamina (SPRL) of *Nagatitan* forms the lateral margin of the spinoprezygapophyseal fossa (SPRF). The spinodiapophyseal lamina (SPDL) is divided into anterior (aSPDL) and posterior (pSPDL) branches. In SM2025-1-546, the aSPDL is vertically orientated and contacts the SPRL close to the base of the neural spine. The pSPDL is also vertically orientated and contacts the spinopostzygapophyseal lamina (SPOL) approximately halfway up the neural spine, close to the ventral margin of the posterior aliform process. The aSPDL of SM2025-1-547 is more prominent dorsoventrally than in SM2025-1-546 and contacts the neural spine at just above midheight. By contrast, the pSPDL of SM2025-1-547 does not contact the SPOL and instead contacts the posterior aliform process, at a slightly dorsoventrally lower point on the neural spine than the dorsal end of the aSPDL. The presence of both an aSPDL and pSPDL has been observed in other somphospondylans, such as *Huabeisaurus*[74] and *Europatitan*[64]. In *Nagatitan*, each SPOL is bifurcated into lateral (lSPOL) and medial (mSPOL) branches throughout its length, represented by low rounded ridges that are directed dorsally. The medial and lateral SPOLs are approximately parallel to each other and are mediolaterally expanded at their ventral and dorsal ends in the posterior dorsal vertebrae. In *Nagatitan*, the lSPOL and the pSPDL extend to converge at the base of the posterior aliform process on the middle neural spine (SM2025-1-546), whereas they appear to converge as they merge into the aliform process in the posterior neural spines (SM2025-1-547 and SM2025-1-548). This character state, wherein the SPDL and especially the lSPOL form part of the posterior aliform process, is also observed in many titanosauriforms, such as *Phuwiangosaurus, Ligabuesaurus* and *Euhelopus*[51,75]. In SM2025-1-546, the left and right mSPOLs merge on the midline near the ventral margin of the neural spine bifurcation. The combined mSPOL then terminates at the contact between the ventromedial margin of the posterior aliform process and the dorsal extent of the neural spine. The mSPOLs of SM2025-1-547 do not merge with each other, but they again terminate close to the ventromedial margins of the posterior aliform processes. SPOLs that are divided throughout their length is otherwise a feature only of rebbachisaurids[61] and as such we regard this as a 'local' autapomorphy (sensu Beeston et al.[76]) of *Nagatitan*. On the posterior face of the neural spine there is a rounded midline spinopostzygapophyseal fossa (SPOF) located just dorsal to the postzygapophyses, bounded by the mSPOLs. The SPOF of SM2025-1-546 tapers dorsally due to the convergence of the mSPOLs. The SPOF of SM2025-1-547 is much more shallow and extends further up the spine as it fades out.

The neural spine flares laterally at its summit, producing well-developed triangular anterior aliform processes in the posteriormost dorsal vertebrae (SM2025-1-547 and SM2025-1-548), and comparably developed posterior aliform processes in all three dorsal vertebrae. Each anterior aliform process is formed by the SPRL and aSPDL, which merge at the ventral margin of the process. The presence of anterior aliform processes has not been observed in any other sauropod. A posterior dorsal vertebra (PW1-27) of *Phuwiangosaurus* appears to exhibit a structure (Suteethorn et al. 2010[49]: Fig. 1 and 2) that could be considered a weakly developed anterior aliform process, but this is not present in other dorsal vertebrae and requires re-evaluation. As such, we regard the presence of anterior aliform processes as an autapomorphy of *Nagatitan*. The posterior aliform process of SM2025-1-546 is triangular and extends further laterally than the postzygapophyses, whereas SM2025-1-547 exhibits weaker triangular aliform processes that do not extend beyond the lateral extent of the postzygapophyses. Posterior aliform processes characterise most eusauropods, except for diplodocoids[7,9]. Within Titanosauriformes, aliform processes that extend beyond the lateral extent of the postzygapophyses are otherwise primarily restricted to brachiosaurids and a small number of titanosaurs[9,50].

Dorsal ribs

Six dorsal ribs (Table 2). Figure 8 have been recovered, although only two have been fully prepared. All six elements probably represent middle or posterior dorsal ribs. SM2025-1-551 is a complete rib, whereas SM2025-1-552 is missing its distal end and has been anteroposteriorly flattened. The capitulum is anteroposteriorly short and oval in proximal view. This process is directed medially and slightly anteriorly from the proximal shaft region. In SM2025-1-551, the capitulum and tuberculum lie in the same vertical plane, making the rib head anteroposteriorly flat. The capitulum articulation is directed ventromedially. In proximal view, the articular surface of the tuberculum is oval in outline. The tuberculum is proximodistally short and facet-like in three specimens, including SM2025-1-551. In SM2025-1-552, the tuberculum is also short but forms a more pronounced facet than in SM2025-1-551. SM2025-1-552 possesses a proximal pneumatic foramen located on its posterior surface, next to the dorsolateral margin of the tuberculum; this indicates that the dorsal ribs are pneumatized, a character state observed in Titanosauriformes[47].

All six ribs exhibit the same shaft morphology, with variation in dimensions. The proximal shaft is subtriangular in cross section, but transforms to a more plank-like cross section at approximately one-third of shaft length from the proximal end, being much longer anteroposteriorly than wide mediolaterally. The anteroposterior to transverse width ratio of SM2025-1-551 is 1.47 at the proximal end of the shaft. This ratio changes in the distal

	Proximodistal length	Proximal head dorsoventral height
SM2025-1*551	1872	225
SM2025-1-552	1672*	487

Table 2. *Nagatitan chaiyaphumensis* gen. et. sp. nov. rib measurements. *Indicates uncertain values due to incomplete or deformed specimen. Measurements in mm.

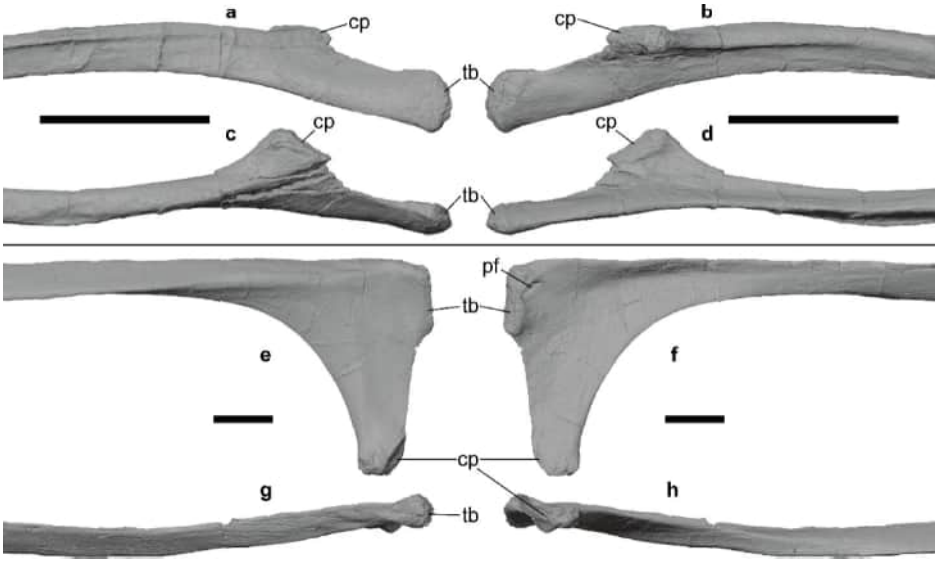

Fig. 8. 3D surface scan model images of dorsal ribs of *Nagatitan chaiyaphumensis* gen. et sp. nov. (**a**–**d**) SM2025-1-551 and (**e**–**h**) SM2025-1-552 in (**a**, **e**) anterior, (**b**, **f**) posterior, (**c**, **g**) dorsal, and (**d**, **h**) ventral views. Scale bars equal 100 mm. cp, capitulum; pf, pneumatic foramen; tb, tuberculum.

third of the shaft to 2.41. The anteroposterior to transverse width ratio of the shaft is significantly higher (4.50) in SM2025-1-552, but this is probably because of deformation of the specimen. On four of the ribs, including both SM2025-1-552 and SM2025-1-551, a narrow but pronounced ridge extends from the anterior surface of the tuberculum and runs along the proximal shaft, decreasing in prominence and disappearing at approximately one third of the way along the shaft distally. In SM2025-1-552 the ridge curves ventrally to merge with the ventral margin of the rib shaft. The distal ventral tip of the rib shaft is rounded.

Sacral vertebrae

Four articulated co-ossified sacral vertebrae and six sacral ribs have been recovered (SM2025-1-550) (Fig. 9). The ventral surface of the sacrum is better preserved than the dorsal surface, although the latter is still under preparation. The posterior margin of the posteriormost preserved centrum is incomplete. It is likely that there is at least one sacral vertebra missing. The anteriormost preserved centrum, interpreted as sacral vertebra 1, is opisthocoelous. It is not possible to determine the internal tissue structure of the sacrum. Moreover, not enough of the lateral surface has been exposed to allow for the identification of lateral pneumatic foramina. All four centra lack midline ventral keels. Only three of the six sacral ribs are well preserved and remain articulated to their corresponding sacral vertebrae. The remaining three are incomplete. Only the ventral acetabular processes of the sacral ribs are exposed. Each acetabular process is anteroposteriorly narrow in its central portion and expands at both ends. The acetabular processes articulate approximately at the middle of their respective centra and are directed laterally. However, the acetabular process of the centrum with the exposed condyle is directed posterolaterally away from the condyle towards the distal symphysis that forms the sacricostal yoke. Only parts of the sacricostal yoke have been preserved on the left and right sides of the specimen. The ventral intercostal foramina formed by the sacral ribs appear to be subcircular, with subacute margins at their lateral and medial ends.

Humerus

The right humerus (SM2025-1-553) (Table 3 and Fig. 10) is complete and undistorted, but is in three pieces. It is a gracile element, with low proximal (0.29), midshaft (0.13), and distal (0.27) mediolateral width to length ratios, and an average value (= Robustness Index of Wilson & Upchurch, 2003)[77] of 0.23. This is broadly similar to the humeral proportions of other early-diverging titanosauriforms, including brachiosaurids, *Ligabuesaurus*, and *Phuwiangosaurus*[7,50], although differing from the proximally broad humerus of *Euhelopus*[78]. There is only a slight lateral expansion of the proximal end of the *Nagatitan* humerus, such that it has an asymmetrical outline in anterior view, as is the case in nearly all titanosauriforms: by contrast, the humerus of other sauropods has an 'hourglass' shape, which also characterises *Euhelopus*[50,79].

Overall, the proximal margin of the *Nagatitan* humerus is convex in anterior view, lacking the strongly sinuous outline of some titanosaurs[75,80]. The proximolateral corner is rounded, differing from the squared morphology that characterises nearly all other somphospondylans[7,81]. As such, we regard this rounded proximolateral corner as a local autapomorphy of *Nagatitan*. The humeral head is off-set medially from the midline of the proximal end. It forms a prominent bulge-like process on the posterior surface of the proximal end. A well-defined ridge extends distally from this posterior process, delimiting the medial and lateral triceps fossae, and fading out at approximately midlength of the humerus. The coracobrachialis fossa is a shallow excavation on the anterior surface of the proximal third of the humerus and contains a low process for the attachment of *M. coracobrachialis*.

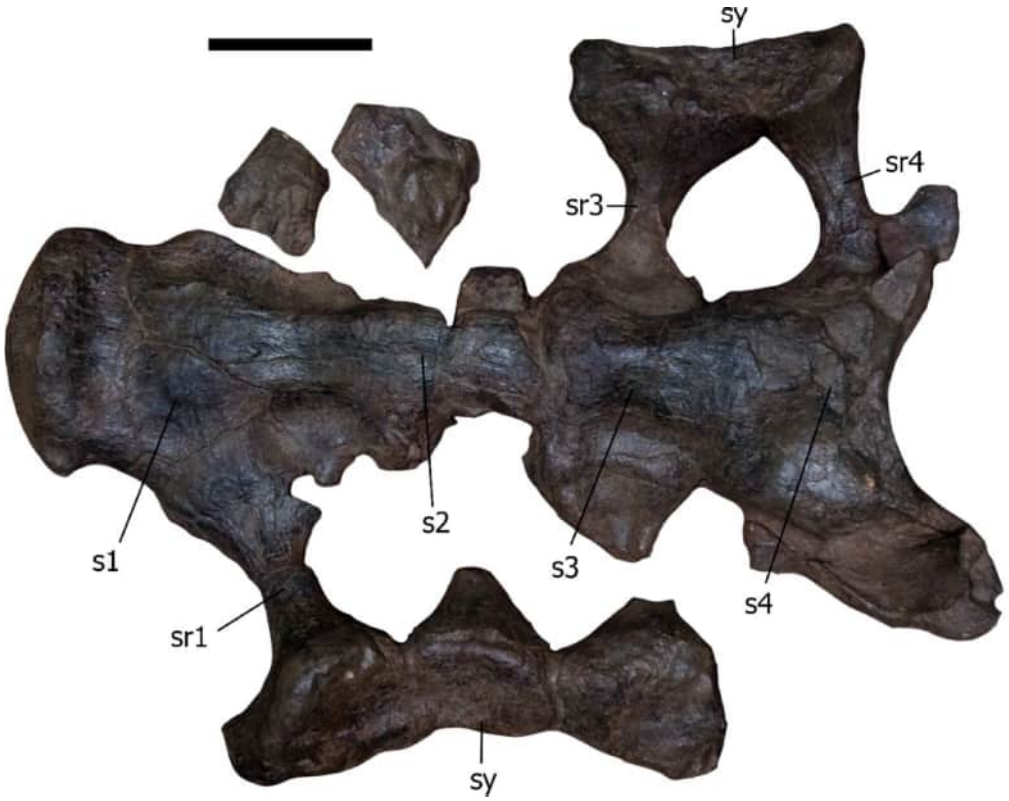

Fig. 9. Photograph of sacrum of *Nagatitan chaiyaphumensis* gen. et sp. nov. (SM2025-1-550) in ventral view. Scale bar equals 200 mm. s, sacral centrum; sr, sacral rib; sy, sacricostal yoke.

	Dimension	Measurement (mm)
Right Humerus	Proximodistal length	1780
	Proximal end maximum mediolateral width	530
	Distance from proximal end to distal tip of deltopectoral crest	860
	Midshaft mediolateral width	236
	Midshaft anteroposterior length	94
	Midshaft minimum circumference	584
	Distal end mediolateral width	484
	Distal end maximum anteroposterior length	214

Table 3. *Nagatitan chaiyaphumensis* gen. et. sp. nov. humerus measurements.

The prominent deltopectoral crest extends along the proximal half of the humerus, terminating at ~ 47% of the element's length. The deltopectoral crest projects anteromedially across the anterior face of the humerus. This orientation characterises numerous titanosauriforms[7], including the East Asian taxon *Fukuititan*[82], although it differs from the condition observed in unequivocal euhelopodids that preserve a humerus, i.e. *Euhelopus*[78] and *Phuwiangosaurus*[12,13], in which the deltopectoral crest projects primarily anteriorly. Unlike some titanosaurs[44,73], the distal deltopectoral crest does not expand mediolaterally in *Nagatitan*. A lateral bulge is located on the posterolateral margin, just proximal to the apex of the deltopectoral crest, which has been interpreted as the insertion site for *M. scapulohumeralis anterior* or *M. deltoideus clavicularis*[83,84]. This is primarily a feature restricted to titanosaurs, although it also occurs in a small number of species outside of this clade, including some brachiosaurids[85]. Given its absence from nearly all early-diverging somphospondylans, including euhelopodids[15,50], we regard its presence in *Nagatitan* as a local autapomorphy. No other bulges or ridges are present on the proximal half of the humerus.

The humeral shaft is considerably wider mediolaterally than anteroposteriorly, producing an elliptical cross-section at midshaft, with an eccentricity value (mediolateral width to anteroposterior depth ratio) of 2.55. This is much greater than in most sauropods, which typically have a humeral eccentricity ranging from 1.3 to 1.8[7,81]. A similarly high eccentricity value has only been documented in a small number of distantly related somphospondylans[7], including *Angolatitan* (2.80) and *Dreadnoughtus* (2.67)[68]. Although it might have been slightly accentuated by anteroposterior crushing in the humerus of *Nagatitan*, we regard high humeral eccentricity

Fig. 10. Photographs and 3D surface scan model images of the right humerus of *Nagatitan chaiyaphumensis* gen. et sp. nov. (SM2025-1-553) in (**a**, **b**) anterior, (**c**, **d**) posterior, (**e**, **f**) lateral, (**g**, **h**) medial, (**i**, **j**) proximal and (**k**, **l**) distal views. Scale bar equals 200 mm. af, anconeal fossa; co, condyle; dpc, deltopectoral crest; hh, humeral head; ltf, lateral triceps fossa; mft, medial triceps fossa; pr, posterior ridge; rac, radial condyle; ulc, ulna condyle.

as a local autapomorphy of the new taxon. As is the case in many somphospondylans[7], the lateral margin of the humeral shaft is straight. This contrasts with the condition in *Euhelopus*[78] and *Phuwiangosaurus*[12,13], in which this margin is concave.

The anterior surface of the distal lateral condyle is divided, forming two ridges. This is the plesiomorphic sauropod condition, whereas this condyle is undivided in titanosaurs and a small number of somphospondylans outside of Titanosauria, including *Tangvayosaurus*[2,7]. In *Nagatitan*, the anconeal fossa is bounded by subvertical supracondylar ridges along the distal third of the posterior surface. The lateral supracondylar ridge is more prominent and acute than the rounded medial ridge, contrasting with the condition in some titanosaurs[85]. The anconeal fossa is relatively shallow in *Nagatitan*, with an anteroposterior depth to that of the remainder of the non-condylar distal humerus ratio of 0.33. This is the plesiomorphic sauropod condition, whereas this ratio is typically 0.4 or greater in many titanosauriforms[7]. Nevertheless, a shallower fossa, comparable to that of *Nagatitan*, also occurs in *Euhelopus* and *Tangvayosaurus*[2,7,85]. Whereas the medial margin of the *Nagatitan* humerus is rounded in distal view, the lateral margin is acute with a posterolaterally deflected surface. A strongly posterolaterally deflected surface is the plesiomorphic eusauropod condition that is lost in nearly all neosauropods[3]: its presence in *Nagatitan* is thus locally autapomorphic within Titanosauriformes. In posterior view, there is a groove along the medial margin above the medial distal condyle.

Ilium

The right ilium (SM2025-1-554) (Table 4 and Fig. 11) is incomplete and broken into five segments. Only the pubic peduncle, ischiadic articulation, and the anterior and ventral portions of the preacetabular blade are preserved. The ilium has also experienced anteroposterior compression, which has slightly deformed the ventral margin of the preacetabulum, increased the angle between the preacetabulum and the pubic peduncle, and heavily deflected the ischiadic articulation posterolaterally from the main body of the ilium.

	Dimension	Measurement (mm)
Right femur	Proximodistal length	1900*
	Proximal end maximum mediolateral width	513
	Proximal end maximum anteroposterior width	220
	Distance from proximal end to distal tip of 4th trochanter	590
	Fourth trochanter proximodistal length	229
	Midshaft mediolateral width	298
	Midshaft anteroposterior length	107
	Midshaft minimum circumference	682
	Distal end mediolateral width	480*
	Distal end maximum anteroposterior length	299*
	Mediolateral breadth of tibial condyle	275*
	Mediolateral breadth of fibular condyle	204*
Right Ilium	Preacetabulum anteroposterior length	490
	Pubic peduncle proximodistal length	423
	Pubic peduncle anteroposterior length	131
	Pubic peduncle mediolateral width	270
	Ischiadic peduncle dorsoventral height	117
	Ischiadic peduncle anteroposterior length	101
	Ischiadic peduncle mediolateral width	201
Right Pubis	Proximodistal length	1194
	Distal end anteroposterior length	435
	Distal end maximum mediolateral width	147
	Iliac peduncle dorsoventral height	245
	Iliac peduncle articular face mediolateral width	146*
	Ischiadic articulation dorsoventral height	539
	Ischiadic articulation mediolateral width	62
	Ischiadic articulation height to pubic proximodistal length	0.45
Left Pubis	Proximodistal length	1042
	Distal end anteroposterior length	417
	Distal end maximum mediolateral width	161
	Iliac peduncle articular face mediolateral width	184
	Ischiadic articulation dorsoventral height	564*
	Ischiadic articulation height to pubic proximodistal length	0.54*

Table 4. *Nagatitan chaiyaphumensis* gen. et. sp. nov. pelvic girdle and femur measurements. *indicates uncertain values due to incomplete or deformed specimen.

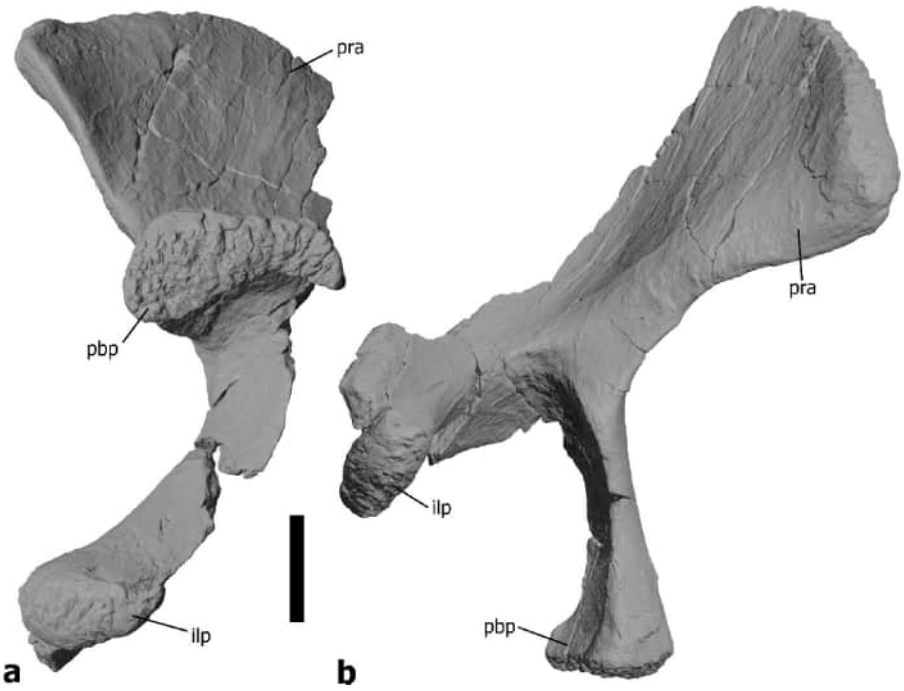

Fig. 11. 3D surface scan model images of the right ilium (SM2025-1-554) of *Nagatitan chaiyaphumensis* gen. et sp. nov. in (**a**) ventral and (**b**) lateral views. Scale bar equals 200 mm. ilp, iliac peduncle; isp, ischiadic peduncle; of, obturator foramen; pbp, pubic peduncle; prap, preacetabular process.

Observing the internal tissue structure through the broken margins of the specimen, the ilium does not exhibit any evidence of pneumatization. As such, it lacks the camellate internal structure that characterises the East Asian early-diverging somphospondylans *Euhelopus*[4], *Ruixinia*[86], and *Tambatitanis*[87], as well as most titanosaurs[7].

The preacetabular process is mediolaterally broad, thickening towards its anteroventral margin, and projects anterolaterally. Unlike the condition in *Phuwiangosaurus*[13], wherein the preacetabular blade is largely vertically oriented, the ventral portion is deflected ventrolaterally in *Nagatitan*. However, the preacetabular process does not form the horizontal shelf observed in some titanosaurs[9]. *Nagatitan* lacks the bulge-like process on the ventral margin of the preacetabular process that is observed in some titanosauriforms[2].

The angle between the ventral margin of the preacetabular blade and the anterior margin of the pubic peduncle is approximately 108°, with the latter process largely perpendicular to the long axis of the ilium, as is the case in nearly all titanosauriforms[1,3]. The gracile pubic peduncle is dorsoventrally tall, such that the ratio between its dorsoventral height and the mediolateral width of its articular surface is 1.57. By comparison, the iliac pubic peduncle of *Phuwiangosaurus*[13] is shorter and more robust, with a ratio of 1.38. In *Nagatitan*, the pubic peduncle is anteroposteriorly short and mediolaterally broad, with a ratio of 0.48 at its distal end, which is similar to most non-titanosaurian titanosauriforms[7]. It has a convex anterior surface and a concave posterior surface, producing a comma-shaped distal end outline.

The ischiadic peduncle is not as well-developed as the pubic peduncle. Although the orientation of the ischiadic peduncle has been distorted, it is likely that it was directed posteroventrally in life. There is some evidence for a notch between the ischiadic peduncle and the posteroventral margin of the postacetabular process, although its morphology cannot be accurately assessed because of distortion.

Pubis

The pubes (SM2025-1-555) (Table 4 and Fig. 12) are preserved in articulation, although they have undergone anteroposterior crushing and mediolateral distortion. Both pubes have been broken into two pieces. The right pubis is complete, whereas the left pubis is missing the majority of the ischiadic articulation.

The ratio between the anteroposterior and mediolateral width of the iliac articular surface is 1.71, although this has been affected by anteroposterior crushing. In lateral view, the proximal surface and proximal third of the anterior margin meet at an acute angle. There is no well-defined ambiens process. The iliac peduncle is confluent with the acetabulum. The elliptical obturator foramen is entirely ringed by bone, as is also the case in most adult sauropods[87]. In *Nagatitan*, the ratio between the dorsoventral height of the ischiadic articulation and the proximodistal length of the pubis is 0.45. Ratios of 0.4 or lower occur in most sauropod clades. However, a ratio higher than 0.4 has been observed in other somphospondylans, including *Tangvayosaurus*[7]. In *Nagatitan*, the symphysis of the pubis appears to be maintained for at least half the length of the distal shaft, starting from the ventral margin of the ischiadic articulation.

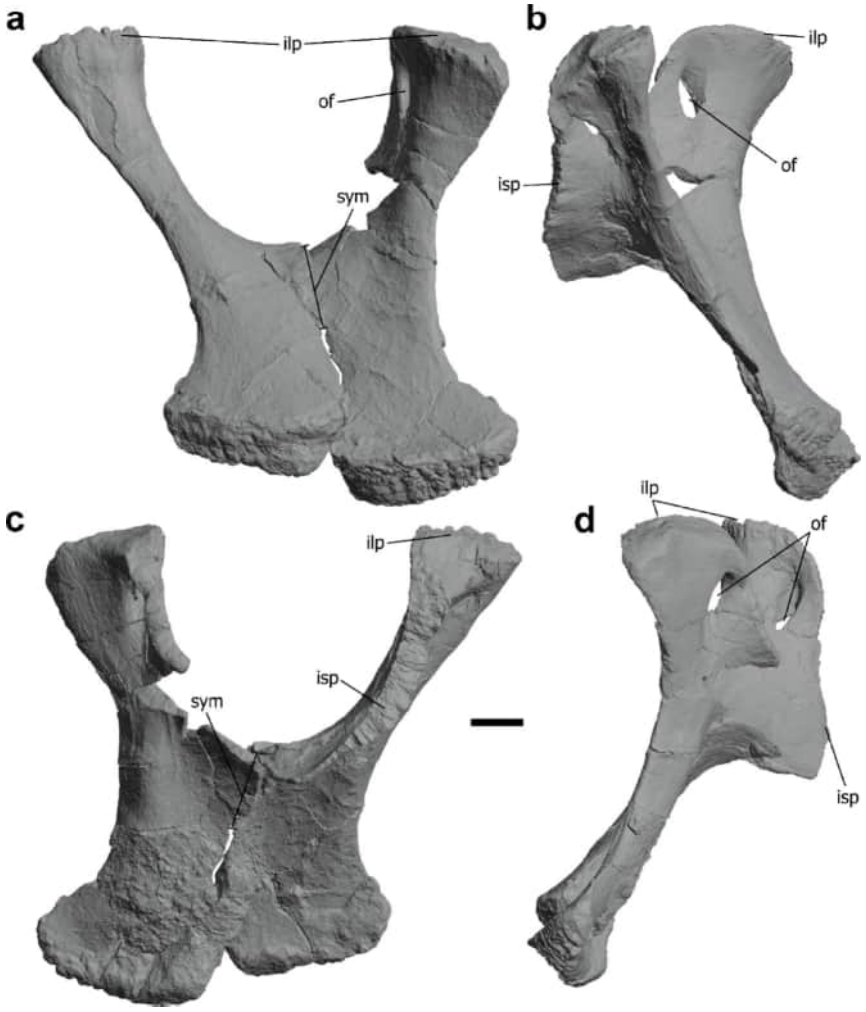

Fig. 12. 3D surface scan model images of the paired pubes (SM2025-1-555) of *Nagatitan chaiyaphumensis* gen. et sp. nov. in (**a**) anterior, (**b**) right lateral, (**c**) posterior, and (**d**) left lateral views. Scale bar equals 200 mm. ilp, iliac peduncle; isp, ischiadic peduncle; of, obturator foramen; pbp, pubic peduncle; prap, preacetabular process; sym, symphysis.

The distal shaft of the pubis is robust and directed anteroventrally. The segment that participates in the symphysis is thin in comparison to the rest of the shaft. The shaft expands laterally at its distal extent. Although this is the plesiomorphic condition in sauropods, it is not observed in most other somphospondylans[50]; therefore, we consider the laterally expanded shaft of the distal end of the pubis as a local autapomorphy for *Nagatitan*. In lateral view, the anterior margin of the distal extent of the shaft is strongly concave, forming a prominent anterior boot: this expansion of the distal end is observed in several other titanosauriforms[7]. In *Nagatitan*, the distal end tapers slightly mediolaterally towards its anterior margin.

Right femur

Only the partial right femur (SM2025-1-556) (Table 4 and Fig. 13), broken into six pieces, has been recovered. A segment of the femoral shaft below the midshaft and the anterolateral portion of the distal end are missing. The fourth trochanter is also incompletely preserved. Despite its incompleteness, the femur shows little to no deformation, with at most some minor anteroposterior compression. We conservatively estimate a proximodistal femoral length of approximately 1.9 to 2 m.

The femoral head is a rounded articulation that is directed dorsomedially, projecting well above the height of the greater trochanter, as in many somphospondylans[9,50], although contrasting with the mainly medially directed femoral head of some euhelopodids, including *Euhelopus*[4], *Phuwiangosaurus*[12,13], and *Tangvayosaurus*[14]. The greater trochanter in *Nagatitan* forms a distinct shelf, separate from the rounded proximal articular head. Proximal to the well-developed lateral bulge, the lateral margin of the femur is medially deflected relative to that of the midshaft, as is the case in most titanosauriforms[7]. The lateral margin of the proximal third anteroposteriorly narrows to form a trochanteric shelf, bounded medially by a rounded ridge that descends from the greater trochanter. This is otherwise primarily a feature of unequivocal titanosaurs and rebbachisaurids[7,88,89], although it also characterises a small number of somphospondylans that probably lie outside of the titanosaur radiation,

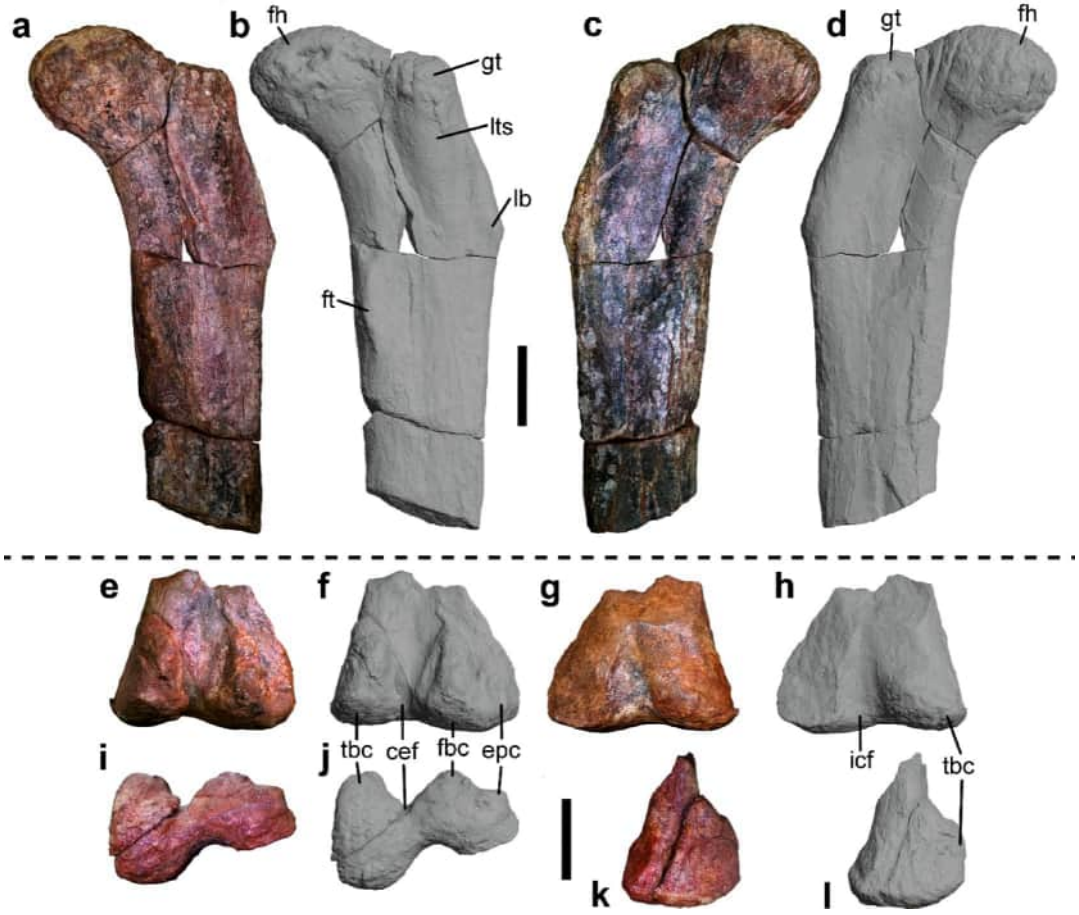

Fig. 13. Photographs and 3D surface scan model images of the (**a**–**d**) proximal and (**e**–**l**) distal segments of the incomplete right femur of *Nagatitan chaiyaphumensis* gen. et sp. nov. (SM2025-1-556) in (**a**, **b**, **e**, **f**) posterior, (**c**, **d**, **g**, **h**) anterior views, (**i**, **j**) distal and (**k**, **l**) medial views. Scale bars equal 200 mm. ef, extensor fossa; epc, epicondyle; fbc, fibular condyle; fh, femoral head; ft, fourth trochanter; gt, greater trochanter; icf, intercondylar fossa; lb, lateral bulge; lts, lateral trochanteric shelf; tbc, tibial condyle.

including *Huabeisaurus*[74] and *Ruyangosaurus*[57]. The partially preserved fourth trochanter is a proximodistally elongate and mediolaterally thin process, and restricted to the medial margin of the posterior surface. Unlike brachiosaurids, and the euhelopodids *Phuwiangosaurus* and *Tangvayosaurus*, the fourth trochanter is not visible in anterior view[7].

The preserved shaft is anteroposteriorly flattened, resulting in an elliptical midshaft cross section with an eccentricity of 2.79. A high eccentricity value (≥ 1.85) characterises the femur of most titanosauriforms[81], although the euhelopodids *Euhelopus* and *Gobititan* are notable exceptions[7]. Values greatly exceeding 2.0 are primarily restricted to titanosaurs[81], although *Phuwiangosaurus* (ecc = 2.6[7,13]) and *Garumbatitan* (ecc = 2.7–3.1[90]) represent non-titanosaurian somphospondylans that share an unusually high femoral eccentricity with *Nagatitan*.

The tibial condyle appears to be anteroposteriorly longer than the fibular condyle, despite the missing anterior face of the latter. The tibial condyle is also narrower mediolaterally than the fibular condyle, with an estimated ratio of 0.74. A ratio of less than 0.8 is commonly observed within titanosauriforms[7,50,81]. In *Nagatitan*, the medial face of the tibial condyle is flat. The posterior surface of the fibular condyle is divided, forming a well-developed epicondyle.

Phylogenetic results

The equal weights (EQW) analysis resulted in 152,064 MPTs with a length of 3008 steps (CI = 0.199, RI = 0.610), producing a well resolved strict consensus tree (Fig. 14). Bremer supports are low across the tree (values of 1–4), with values of 1 or 2 for all euhelopodids and most somphospondylans. Average Branch support of the EQW results is 0.7. Relationships are broadly consistent with recent iterations of this data matrix[91]. Using the definition provided by D'Emic[2], Euhelopodidae contains *Nagatitan, Europatitan, Phuwiangosaurus, Tangvayosaurus, Jiangshanosaurus, Qiaowanlong, Yongjinglong, Euhelopus, Erketu* and *Gobititan*. *Nagatitan* is placed as the sister taxon to *Europatitan*, supported by the shared presence of anterior spinodiapophyseal laminae (aSPDL) on the middle–posterior dorsal neural spines. *Phuwiangosaurus* remains as the sister taxon of *Tangvayosaurus*,

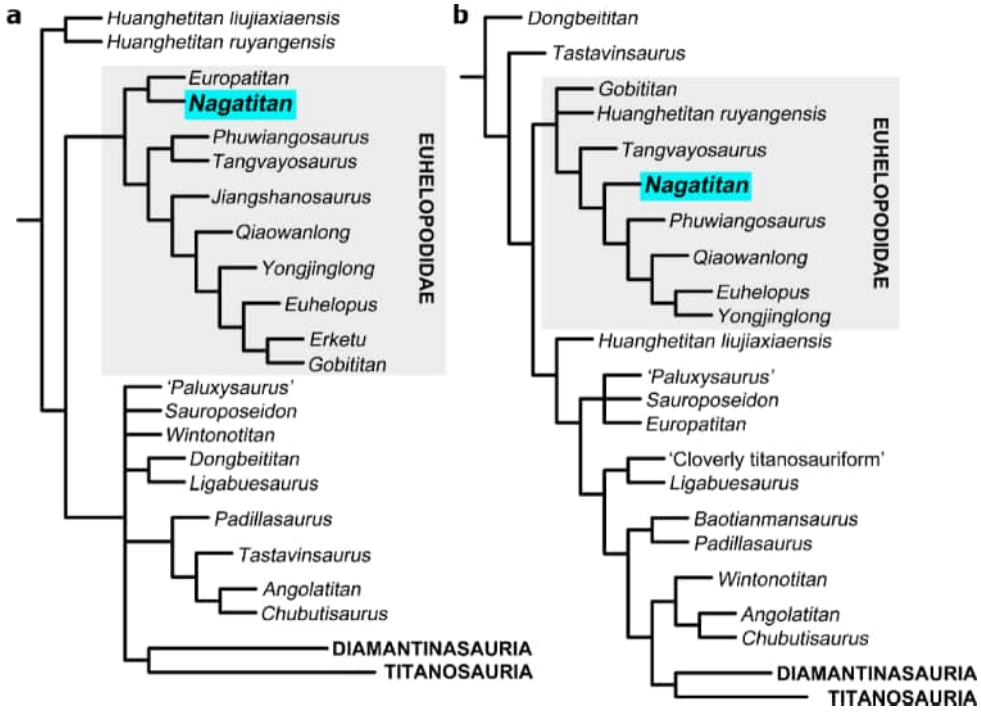

Fig. 14. Strict consensus trees showing the systematic position of *Nagatitan chaiyaphumensis* gen. et. sp. nov. among somphospondylan sauropod dinosaurs generated under (**a**) equal character weighting and (**b**) extended implied weighting.

as observed in previous iterations of the matrix[3,7,8,15,50,67,91]. *Nagatitan* + *Europatitan* is the sister taxon to the lineage containing *Phuwiangosaurus* + *Tangvayosaurus* and the remaining members of Euhelopodidae.

Under extended implied weighting (EIW), the analysis yields 24,300 MPTs with a length of 123.96 steps (CI = 0.191, RI = 0.590), resulting in a generally well resolved strict consensus tree (Fig. 14). Euhelopodidae is better resolved in the strict consensus tree produced in this study than in the most recent iteration of the data matrix[91]. Euhelopodidae contains *Gobititan* and *Huanghetitan ruyangensis* in a polytomy at the 'base' of the clade, with the following taxa successively more phylogenetically nested: *Tangvayosaurus, Nagatitan, Phuwiangosaurus, Qiaowanlong, Euhelopus* and *Yongjinglong*. Unlike the EQW results, *Europatitan* forms a polytomy with '*Paluxysaurus*' and *Sauroposeidon*. *Erketu* is no longer part of Euhelopodidae, and instead is now placed within a polytomy containing *Andesaurus, Dongyangosaurus* and *Huabeisaurus*. *Jiangshanosaurus* is also positioned in a large polytomy within Titanosauria. The recovery of *Nagatitan* within Euhelopodidae is supported by three synapomorphies: (1) the ratio between the dorsoventral height of the neural spine and posterior centrum of the posterior dorsal vertebra is less than 1.0; (2) the SPOLs of the middle and posterior dorsal neural spines are divided into lateral and medial branches; and (3) the lateral margin of the humeral diaphysis is straight.

Body size and mass estimates

We obtained an estimated body mass of approximately 27 tonnes, with a body length of 27 m for *Nagatitan* (Table 5). These body size and mass estimates are substantially higher than those calculated based on limb circumferences obtained from the holotype individual of *Phuwiangosaurus* (~12 tonnes, 15 m in length). The estimated body mass and length of the *Tangvayosaurus* holotype individual is approximately 23 tonnes and 24 m in length, close to that of *Nagatitan*. In comparison with other East and Southeast Asian somphospondylan taxa (Table 5), *Nagatitan* has an estimated body mass similar to that of *Gobititan, Tangvayosaurus, Fusuisaurus, Opisthocoelicaudia, Jiangshanosaurus*, and *Huabeisaurus* .

Discussion

Relationships with other Southeast Asian taxa

Both of our phylogenetic analyses support a euhelopodid somphospondylan placement for *Nagatitan*, with the Southeast Asian taxa, *Phuwiangosaurus* and *Tangvayosaurus*, also part of this clade. Our detailed description, comparisons, and phylogenetic analyses demonstrate that *Nagatitan* can be diagnosed by two autapomorphies, in addition to a unique character combination. It also does not form a clade with *Phuwiangosaurus* and *Tangvayosaurus* to the exclusion of other euhelopodids, suggesting that these three taxa are not part of an endemic subclade. Below, we make detailed anatomical comparisons between *Nagatitan* and these two taxa to better illustrate how they differ.

Taxon	Horizon and age	HC	FC	Body mass (kg)	Body length (m)
Opisthocoelicaudia (Borsuk-Białynicka 1977; ZPAL MgD-1/48)	Nemegt Formation Maastrichtian	465	650	18,748	21.37
Zhuchengtitan (Mo et al. 2017; ZJZ-57)	Xingezhuang Formation Campanian	623*	763**	34,096	32.19
Sonidosaurus (Xu et al. 2006)	Iren Dabasu Formation Campanian	–	–	5,303***	~9
Jiangshanosaurus (Tang et al. 2001; Mannion et al. 2019b; ZMNH M1322)	Jinhua Formation Turonian–Coniacian	532*	650	22,010	23.85
Qingxiusaurus (Mo et al. 2008; NHMG 8499)	Unnamed unit Cenomanian–Maastrichtian?	405+	493**	10,345++	14.22
Huabeisaurus (Pang and Cheng 2000; D'Emic et al. 2013; HBV-20001)	Huiquanpu Formation Cenomanian–Campanian	528*	645	21,553	23.51
Gandititan (Han et al. 2024)	Zhoutian Formation Cenomanian–Turonian	–	–	10,108***	~14
Borealosaurus (You et al. 2004; LPM0170)	Sunjiawan Formation Albian	318	386*	5,294	8.99
Gobititan (You et al. 2003; IVPP 12,579)	Zhonggou Formation Albian	536*	655	22,476	24.20
Fusuisaurus (Mo et al. 2020; LCL 63)	Xinlong Formation Aptian–Albian	605	741*	31,446	30.46
Nagatitan (This study; SM2025-1-553, 556)	Khok Kruat Formation Aptian– Albian	584	682	26,582	27.15
Ruyangosasurus (Lü et al. 2009; 41HIII-0002)	Haoling Formation Aptian–Albian	732*	905	53,996	44.10
Xianshanosaurus (Lü et al. 2009; KLR-0762-15)	Haoling Formation Aptian–Albian	476*	580	16,164	19.31
Tangvayosaurus (Allain et al. 1999, TV4)	Grès supérieurs Formation Aptian–Albian	541*	661	23,022	24.60
Fukuititan (Azuma and Shibata 2010; FPDM-V8468)	Kitadani Formation Barremian–Aptian	365	445	7,787	11.71
Daxiatitan (You et al. 2008; GSLTZP03-001)	Hekou Group Barremian	517**	631+	20,298++	22.57
Dongbeititan (Wang et al. 2007; D2867)	Yixian Formation Barremian	489**	596+	17,389++	20.30
Liaoningotitan (Zhou et al. 2018)	Yixian Formation Barremian	–	–	6,184***	~10
Phuwiangosaurus (Martin et al. 1994; PW 1)	Sao Khua Formation Valanginian–Barremian	364	551	10,888	15.40
Hamititan (Wang et al. 2021)	Shengjinkou Formation Valanginian	–	–	13,420***	~17
Euhelopus (Wiman 1929; Young 1935; Wilson & Upchurch 2009; PMU 233)	Mengyin Formation Berriasian–Valanginian	358	375	5,924	9.71

Table 5. List of titanosauriforms from Asia with body mass and body length estimates ordered by stratigraphic age. HC, humeral circumference; FC, femoral circumference. An asterisk (*) indicates limb bone circumference value estimated based on methods from Benson et al. (2018), using minimum shaft mediolateral width. A double asterisk (**) indicates that the limb bone circumference value was estimated based on methods from Benson et al. (2018), using an estimated circumference value of another limb bone based on its mediolateral width. A triple asterisk (***) indicates body mass estimated from body length using the method presented by Seebacher (2011). A plus symbol (+) indicates limb bone circumference value estimated based on Ramanujan's second approximation. A double plus symbol (++) indicates a body mass estimate derived from limb bone circumferences estimates made using Ramanujan's second approximation.

Phuwiangosaurus is known from the upper Valanginian–Barremian (Lower Cretaceous) Sao Khua Formation of Thailand, with specimens from multiple localities assigned to this taxon[12,13,48,49]. Shared skeletal elements between *Nagatitan* and *Phuwiangosaurus* comprise: middle–posterior dorsal vertebrae, dorsal ribs, sacrum, humerus, ilium, pubis, and femur. *Nagatitan* differs from *Phuwiangosaurus* in numerous anatomical features: (1) two hyposphene morphologies are present in *Nagatitan,* whereas *Phuwiangosaurus* exhibits only the triangular morphology; (2) *Nagatitan* exhibits paired, sharp-lipped shallow fossae on the anterior surface of posterior dorsal neural arches, dorsolateral to neural canal and medial to CPRLs, which are absent in *Phuwiangosaurus;* (3) the parapophyses are positioned dorsal to the prezygapophyses on the posterior dorsal neural arches in *Nagatitan*, but are ventral or level with them in *Phuwiangosaurus;* (4) the middle–posterior dorsal diapophyses of *Nagatitan* are directed both above and below 45°, whereas in *Phuwiangosaurus* they are all directed at 45° or greater; (5) an aSPDL is present on the middle–posterior dorsal neural spines of *Nagatitan*, but is absent in *Phuwiangosaurus*; (6) the SPOLs of *Nagatitan* are divided, whereas they are undivided in *Phuwiangosaurus*; (7) the aliform process of the middle dorsal neural spines are strongly developed in *Nagatitan*, but weakly

developed in *Phuwiangosaurus*; (8) middle dorsal neural spines are bifurcated in *Nagatitan*, but bifurcation is restricted to anterior dorsal neural spines in *Phuwiangosaurus;* (9) the proximolateral corner of the humerus is rounded in *Nagatitan* and squared in *Phuwiangosaurus*; (10) a pronounced bulge on the lateral margin of the posterior humeral surface, level with the most developed portion of the deltopectoral crest, characterizes *Nagatitan*, but is absent in *Phuwiangosaurus;* (11) the deltopectoral crest is directed anteromedially in *Nagatitan* and anteriorly in *Phuwiangosaurus*; (12) the lateral margin of the humeral diaphysis is straight in *Nagatitan* but concave in *Phuwiangosaurus;* (13) a ventral bulge on the preacetabular process of the ilium is lacking in *Nagatitan*, but present in *Phuwiangosaurus;* (14) the iliac articular surface of the pubis is anteroposteriorly shorter in *Nagatitan* (anteroposterior to mediolateral diameter ratio of 1.71) than in *Phuwiangosaurus* (2.2); (15) the femoral head is directed dorsomedially in *Nagatitan* and medially in *Phuwiangosaurus*; and (16) the fourth trochanter is not visible in anterior view in *Nagatitan*, unlike in *Phuwiangosaurus*. In our body size estimation of *Phuwiangosaurus*, two factors should be noted. Firstly, the holotype humerus and femur do not represent the largest limb specimens attributed to the taxon, with additional elements approximately 10% longer; secondly, osteohistological studies demonstrate that the holotype humerus has a histological ontogenetic stage of 12, with a maximum of 13 stages for sauropods[92]. This indicates that the holotype material likely did not originate from a fully grown individual. Nevertheless, it is difficult to conceive that these factors could explain the difference in our body mass estimates, with that of *Nagatitan* exceeding *Phuwiangosaurus* by approximately 10 tonnes.

Tangvayosaurus is known from the Aptian–Albian Grés supérieurs Formation of Laos, with remains from two localities[14]. Shared skeletal elements between *Nagatitan* and *Tangvayosaurus* comprise: middle dorsal vertebrae, dorsal ribs, humerus, ilium, pubis, and femur. *Nagatitan* differs from *Tangvayosaurus* in several aspects: (1) the posterior articular surfaces of middle dorsal centra are mediolaterally wider than dorsoventrally tall in *Nagatitan*, whereas the reverse is true in *Tangvayosaurus*; (2) an aSPDL is present in the middle dorsal vertebrae of *Nagatitan* but absent in *Tangvayosaurus*; (3) the dorsal neural spine is shorter than the posterior dorsoventral height of the centrum in *Nagatitan* compared to *Tangvayosaurus*; (4) the anterior surface of the humeral distal lateral condyle is divided in *Nagatitan*, but undivided in *Tangvayosaurus*; (5) the femoral head of *Nagatitan* is directed dorsomedially, whereas it is directed medially in *Tangvayosaurus*; (6) the fourth trochanter is not visible in anterior view in *Nagatitan,* unlike that in *Tangvayosaurus*; and (7) the lateral margin of the proximal third of the femur of *Nagatitan* narrows anteroposteriorly to form a flange-like trochanteric shelf, whereas it remains relatively constant in *Tangvayosaurus*. Unlike *Phuwiangosaurus*, the estimated body mass for *Tangvayosaurus* is similar to that of *Nagatitan*.

One caveat is that the current character matrix scoring for both *Phuwiangosaurus* and *Tangvayosaurus* is not based on first-hand observation. Notably, *Tangvayosaurus* has yet to receive a detailed description, with only a brief report currently published[14], although the scores for this taxon were supplemented with photographs of the material[7]. Both the holotype and referred material of *Phuwiangosaurus* have received a detailed description[12,13,48,49,93], although it is unclear whether all of these specimens can be confidently attributed to a single genus and there remains a possibility that *Phuwiangosaurus* has become a 'waste basket' taxon for Cretaceous titanosauriform material from Thailand. As such, the interrelationships of *Nagatitan*, *Phuwiangosaurus* and *Tangvayosaurus*, along with their relationships with East Asian euhelopodids, might change in the future with the incorporation of first-hand observations and taxonomic re-evaluations.

Faunal similarities with the Xinlong Formation

The vertebrate assemblage from the Khok Kruat Formation has been suggested to be similar to that of the Aptian–Albian Xinlong Formation that outcrops in Guangxi, southern China[18,35]. Two titanosauriform species are currently known from the latter formation, *Fusuisaurus*[23,94] and *Liubangosaurus*[24,95]. The phylogenetic affinities of both of these taxa are uncertain, although it seems likely that they represent somphospondylan titanosauriforms, with some evidence for euhelopodid affinities[2,7,23,24,95]. *Fusuisaurus* shares the following skeletal elements with *Nagatitan*: dorsal ribs, humerus, ilium, pubis, and the distal end of the femur[23,94]. It differs from *Nagatitan* in the following aspects: (1) the dorsal ribs of *Nagatitan* are pneumatised, whereas those of *Fusuisaurus* are not; (2) the deltopectoral crest is directed anteromedially in *Nagatitan*, whereas it is directed anteriorly in *Fusuisaurus*; and (3) the distal end of the pubis of *Nagatitan* is transversely expanded, whereas that of *Fusuisaurus* has a laminar distal blade. *Fusuisaurus* exhibits some similarities to *Nagatitan*, most notably the rounded proximolateral corner of the humerus, which is only observed in a few somphospondylans[8].

Liubangosaurus[24] overlaps with *Nagatitan* only in the preservation of middle–posterior dorsal vertebrae, and differs in the following aspects: (1) the posterior articular surfaces of middle dorsal centra are mediolaterally wider than dorsoventrally tall in *Nagatitan*, whereas the reverse is true in *Liubangosaurus*; (2) the lateral pneumatic foramina are set within a lateral fossa in *Nagatitan*, whereas *Liubangosaurus* has pneumatic foramina that are flush with the lateral surface of the centrum; (3) the middle–posterior dorsal anterior neural canal of *Nagatitan* is entirely surrounded by the neural arch and is enclosed in a deep fossa, whereas *Liubangosaurus* only possesses the latter morphology; (4) *Nagatitan* exhibits paired shallow excavations dorsolateral to the neural canal and medial to the CPRLs, whereas *Liubangosaurus* lacks this feature entirely; (5) two hyposphene morphologies are present in *Nagatitan,* whereas *Liubangosaurus* exhibits only the triangular morphology; (6) the posterior dorsal parapophysis of *Nagatitan* is positioned dorsal to the prezygapophysis, whereas in *Liubangosaurus* it is level with the prezygapophysis; (7) the PCDL of *Nagatitan* is unexpanded at its ventral tip, unlike that of *Liubangosaurus* which is expanded and bifurcates; (8) *Nagatitan* possesses an aSPDL, whereas *Liubangosaurus* lacks this feature; (9) the middle–posterior dorsal diapophyses of *Nagatitan* display serial variation in their orientations (i.e. directed dorsolaterally above 45° in the middle dorsal vertebrae and below 45° in the posterior ones), whereas they are all directed dorsolaterally above 45° in *Liubangosaurus*; (10) the dorsal neural spine of *Nagatitan* has approximately constant anteroposterior width along its dorsoventral height, whereas *Liubangosaurus* has a neural spine that narrows dorsally so that it is triangular in lateral view; (11) the SPOLs of *Nagatitan* are divided,

whereas they are undivided in *Liubangosaurus*; and (12) the aliform processes of the middle dorsal neural spines are strongly developed in *Nagatitan*, but weakly developed in *Liubangosaurus*.

At present, there is no evidence to suggest close affinities between *Nagatitan* and either of the titanosauriforms of the Xinlong Formation, despite the apparent similarities between non-dinosaurian vertebrates from this fauna and that of the Khok Kruat Formation.

A European euhelopodid?

The results from our phylogenetic analysis with EQW recover *Nagatitan* as the sister taxon of *Europatitan eastwoodi*, which is known from a partial skeleton from the upper Barremian–lower Aptian Castrillo de la Reina Formation of Spain[64]. If correct, *Europatitan* would represent a euhelopodid from outside of Asia, casting doubt on the apparent endemicity of this somphospondylan clade. Previous evidence for purported euhelopodids outside of Asia are limited to isolated teeth from a contemporaneous Spanish deposit[96]. The Castrillo de la Reina Formation shares some broad faunal similarities with the Khok Kruat Formation based on the presence of iguanodontians and spinosaurids[97,98]. Skeletal elements present in both *Europatitan* and *Nagatitan* include: a middle–posterior dorsal vertebrae, dorsal ribs, and the pubis. The two taxa share the presence of anterior spinodiapophyseal laminae (aSPDL) on the middle–posterior dorsal neural spines, which is recovered as a synapomorphy of this clade in our EQW analysis. However, *Nagatitan* differs from *Europatitan* in the following respects: (1) the lateral pneumatic foramina in the dorsal centra of *Nagatitan* are not divided by internal ridges, such as those present in *Europatitan*; (2) *Nagatitan* possesses two hyposphene morphologies, whereas *Europatitan* only exhibits the triangular hyposphene morphology; (3) the parapophyses are positioned dorsal to the prezygapophyses on the posterior dorsal neural arches in *Nagatitan*, but they are ventral to (or level with) the prezygapophyses in *Europatitan*; (4) the middle–posterior dorsal diapophyses of *Nagatitan* display serial variation in their orientations (i.e. directed dorsolaterally above 45° in the middle dorsal vertebrae and below 45° in the posterior ones), whereas they are all directed dorsolaterally in *Europatitan*; (5) the ACDL is present in *Nagatitan* but absent in *Europatitan*; (6) the CPRLs are undivided in *Nagatitan* but are bifurcated in *Europatitan*; (7) the middle dorsal vertebral SPOLs of *Nagatitan* are divided throughout their length, unlike those of *Europatitan*; (8) the pubis of *Nagatitan* exhibits an anteriorly expanded 'boot' at its distal end, which is absent in *Europatitan*; and (9) the distal end of the pubis also expands transversely relative to the shaft in *Nagatitan* but does not in *Europatitan*. These anatomical differences are reflected in the results of our EIW analysis, in which *Europatitan* lies outside of Euhelopodidae. Thus, we regard it as premature to consider that the euhelopodid clade was present outside Asia.

Titanosauriform body size evolution in Asia

The evolutionary maximum body size of sauropods rapidly increased early on in their evolutionary history, before plateauing[99–102]. D'Emic[102] demonstrated that certain sauropod clades exhibited decreasing body mass trends, including Titanosauriformes (see also Souza and Santucci[103]). Despite this, many sauropods from the middle and Late Cretaceous are characterised by extremely high body mass estimates (> 40 tonnes), including *Argentinosaurus*, *Notocolossus, Patagotitan*, and *Ruyangosaurus*[56,68,75,101,104,105].

Although *Nagatitan* is not the largest titanosauriform from Asia, it is currently the largest taxon known from Southeast Asia, with an estimated body mass exceeding 26 tonnes (Fig. 15). When comparing body mass estimates of Asian titanosauriforms, pre-Aptian species have an average body mass of approximately 9 tonnes and, with the exception of *Daxiatitan*, none have been estimated to exceed 20 tonnes (Table 5). However, most titanosauriforms present from the Aptian onwards exceed 20 tonnes, with *Ruyangosaurus* the largest species[56], with an estimated body mass of over 50 tonnes (Table 5).

Distinct outliers in our dataset include the Late Cretaceous taxa *Sonidosaurus*[106] and *Gandititan*[6], with estimated body masses of approximately 5 and 10 tonnes, respectively, although neither of these species preserve a humerus or femur, and their ontogenetic stage is unknown. It appears that titanosauriforms in Asia began increasing their maximum body mass during the middle Cretaceous, before settling into a much wider range of masses in the Late Cretaceous.

Sewall et al.[107] suggested that Southeast Asia was dominated by forest-, savannah- and shrubland-like environments during the Aptian–Albian, due to its position between the midlatitudes and the Equator. Previous studies of the Khok Kruat Formation have noted the presence of caliche pebble conglomerates which could indicate an arid to semi-arid subtropical climate, providing further evidence that, at the very least, parts of the palaeoenvironment during the Aptian–Albian in Southeast Asia were savannah- or shrubland-like[18]. Upchurch and Chiarenza[108] suggested that sauropods were probably able to tolerate and even thrive in higher environmental temperatures[99,109,110]. The rise of global temperatures from the Aptian to the Cenomanian–Turonian Thermal Maximum (CMT) might not have directly driven the body mass diversification, but contributed to the trend towards savanna-like arid environments[111], which favours large primary consumers such as sauropods[112]. This would have allowed niche-filling and the evolutionary cascade model[100] to drive diversification of sauropod body sizes from the middle Cretaceous onwards.

Methods

Surface scanning

Three-dimensional surface scans of the specimens were made using an Artec Space Spider 3D scanner, creating a digital mesh (Artec 3D, Santa Clara, CA, USA; www.artec3d.com/portable-3dscanners/artec-spider-v2). The scans were subsequently processed in Artec Studio Professional v16 (www.artec3d.com/3d-software/artec-studio) to create 3D models in STL formats (see Supplementary 2).

Fig. 15. Stylized life reconstruction of *Nagatitan chaiyaphumensis* gen. et. sp. nov. within the arid floodplains of late Early Cretaceous Aptian–Albian Thailand illustrated by Patchanop Boonsai.

Phylogenetic approach

Nagatitan was incorporated into the data matrix of Díez Díaz et al.[91], which contains 570 characters and 153 taxa, and is the most recent iteration of a data matrix initially developed by Mannion et al.[7], with several substantial expansions (e.g.,[3,50]). Phylogenetic analysis was carried out under a Parsimony framework in TNT v. 1.6[113]. Analyses were run with equal character weighting (EQW) and extended implied weighting (EIW)[114,115], with the latter using a *k*-value of 9, consistent with the approach used by Díez Díaz et al.[91] and appropriate for a matrix of this size[116]. Following the latest iteration of the matrix[91], 17 of the 570 characters were treated as ordered (characters 11, 14, 15, 27, 40, 51, 104, 147, 148, 195, 205, 259, 297, 426, 435, 472 and 510). Sixteen highly unstable OTUs were excluded a priori for the EQW analysis (*Arrudatitan, Astrophocaudia, Australodocus, Brontomerus, Caieiria,* 'Cloverly titanosauriform', *Fukuititan, Fusuisaurus, Liubangosaurus, Malarguesaurus, Mongolosaurus, Paralititan, Puertasaurus, Ruyangosaurus, Shingopana,* and *Trigonosaurus*) and eight for the EIW analysis (*Astrophocaudia, Australodocus, Brontomerus, Fukuititan, Fusuisaurus, Liubangosaurus, Malarguesaurus,* and *Mongolosaurus*). Both analyses were conducted using the New Technology Search with Drift, Sectorial Searches, and Tree Fusing enabled. The consensus was stabilized five times before the resultant trees were used as starting points for a 'Traditional Search' employing Tree Bisection-reconnection.

Body size estimation approach

Body mass estimations were calculated for *Nagatitan* and other Southeast East and Asian titanosauriforms using the equations presented in Benson et al.[104] for quadrupeds, which uses the combined minimum shaft circumference of the humerus and femur (H+F) in millimetres to find body mass (M) in kilograms:

$$\mathrm{M} = \frac{102.749\ \log\ (\mathrm{H} + \mathrm{F})\ \text{-}\ 1.104}{1000}$$

To estimate body mass, taxa must preserve either a humerus or femur where the minimum shaft circumference (HC and FC) or minimum mediolateral shaft width (HML and FML) has been recorded. The minimum mediolateral shaft width is used to estimate the minimum shaft circumference using the equations from Benson et al.[104]. If only one of the required limb bone circumferences was obtained, the value was used to estimate the missing minimum shaft circumferences. The minimum shaft circumference equations are as follows:

To find the minimum circumference of the femur

$$\log_{10}(\mathrm{FC}) = 1.014 \times \log_{10}(\mathrm{HC}) + 0.049$$
$$\log_{10}(\mathrm{FC}) = 0.961 \times \log_{10}(\mathrm{FML}) + 0.508$$

To find the minimum circumference of the humerus

$$\log_{10}(\mathrm{HC}) = 0.969 \times \log_{10}(\mathrm{FC})$$
$$\log_{10}(\mathrm{HC}) = 0.900 \times \log_{10}(\mathrm{HML}) + 0.667$$

In cases where the anteroposterior width of the shaft could also be obtained alongside the mediolateral width to estimate a limb circumference, we utilize the Ramanujan's second approximations[117] in addition to Benson et al.[104]. Ramanujan's second approximations has previously been utilized in studies involving the limb bone[118,119] and LAG circumference[120] of ornithischian dinosaurs. The equation utilizes the radius on the long and short (a and b) perpendicular axes of the ellipses to approximate its circumference:

$$C \approx \pi (a+b)\left(1+\frac{3h}{10+\sqrt{4-3h}}\right)$$

where $h=\frac{(a-b)^2}{(a+b)^2}$.

Using the mediolateral width of the shaft to estimate minimum shaft circumference results in an overestimated or underestimated circumference value (and therefore an overestimated or underestimated body mass), depending on the method used. For example, using the mediolateral width of the humeral shaft of *Nagatitan*, we estimate a minimum circumference value of approximately 635 mm and 543 mm (see Supplementary 3), based on the methods of Benson et al.[104] and Ramanujan[117], respectively, in comparison to the actual value of 584 mm. When estimating the minimum shaft circumference of the femur, this results in values of 769 mm and 672 mm in comparison to the actual value of 682 mm. Typically, the method described by Benson et al.[104] produces an error margin of ± 12% for estimating minimum humeral shaft circumference and ± 7% for the femur (see Supplementary 3). In one extreme case (*Euhelopus*) we find an overestimation of 35% for the humerus. This results in body mass estimation error margin of ± 22%. Ramanujan's approximation typically results in humeral and femoral circumference estimations that are closer to the actual circumference with an error margin of ± 4% and ± 3% respectively. As a result, body mass estimated using the circumferences derived from Ramanujan's approximation have an error margin of roughly ± 9%. Based on these results, we consider Ramanujan's[117] method to be a more accurate approach for estimating minimum limb bone circumference. However, it is limited because it requires an anteroposterior shaft width, which is often absent in taxonomic studies, especially older publications. In contrast, mediolateral widths are more commonly reported. In our study we continue to apply the Benson et al.[104] method to estimate minimum shaft circumference where a true measurement or Ramanujan[117] method cannot be applied.

Body length estimates (Table 5) were calculated using the equation proposed by Seebacher[121]:

$$\mathrm{M} = 214.44\mathrm{L}^{1.46}$$

where L = body length in meters. In addition to body mass calculations made using the method from Benson et al.[104], we have also included body mass estimates for taxa that have estimated body length in previous publications. These body mass calculations were made with the body length Eq. [121] presented above.

Data availability

The data that support the findings of this study are available from the corresponding author upon reasonable request.

Received: 15 December 2025; Accepted: 31 March 2026
Published online: 14 May 2026

References

1. Salgado, L., Coria, R. A. & Calvo, J. O. Evolution of titanosaurid sauropods. I: Phylogenetic analysis based on the postcranial evidence. *Ameghiniana* **34**, 3–32 (1997).
2. D'Emic, M. D. The early evolution of titanosauriform sauropod dinosaurs. *Zool. J. Linn. Soc.* **166**, 624–671 (2012).
3. Mannion, P. D., Upchurch, P., Schwarz, D. & Wings, O. Taxonomic affinities of the putative titanosaurs from the Late Jurassic Tendaguru Formation of Tanzania: Phylogenetic and biogeographic implications for eusauropod dinosaur evolution. *J. Syst. Palaeontol.* **185**, 784–909 (2019).
4. Wilson, J. A. & Upchurch, P. Redescription and reassessment of the phylogenetic affinities of *Euhelopus zdanskyi* (Dinosauria: Sauropoda) from the Early Cretaceous of China. *J. Syst. Palaeontol.* **7**, 199–239 (2009).
5. Wang, X. et al. The first dinosaurs from the Early Cretaceous Hami Pterosaur Fauna, China. *Sci. Rep.* **11**, 14962 (2021).
6. Han, F. et al. A new titanosaurian sauropod, *Gandititan cavocaudatus* gen. et sp. nov., from the Late Cretaceous of southern China. *J. Syst. Palaeontol.* **22**, 2293038 (2024).
7. Mannion, P., Upchurch, P., Barnes, R. & Mateus, O. Osteology of the Late Jurassic Portuguese sauropod dinosaur *Lusotitan atalaiensis* (Macronaria) and the evolutionary history of basal titanosauriforms. *Zool. J. Linn. Soc.* **168**, 98–206 (2013).
8. Moore, A. J., Upchurch, P., Barrett, P. M., Clark, J. M. & Xing, X. Osteology of *Klamelisaurus gobiensis* (Dinosauria, Eusauropoda) and the evolutionary history of Middle–Late Jurassic Chinese sauropods. *J. Syst. Palaeontol.* **18**, 1299–1393 (2020).
9. Upchurch, P. The phylogenetic relationships of sauropod dinosaurs. *Zool. J. Linn. Soc.* **124**, 43–103 (1998).
10. Upchurch, P., Barrett, P. M. & Dodson, P. Sauropoda. in *The Dinosauria, Second Edition* 259–324 (2004).
11. Royo-Torres, R., Cobos, A. & Alcalá, L. A giant European dinosaur and a new sauropod clade. *Science* **314**, 1925–1927 (2006).
12. Martin, V., Buffetaut, E. & Suteethorn, V. A new genus of sauropod dinosaur from the Sao Khua formation (Late Jurassic or Early Cretaceous) of northeastern Thailand. *Comptes Rendus Acad. Sci. Ser. II Sci. Terre Planetes* **3**, 1085–1092 (1994).
13. Martin, V., Suteethorn, V. & Buffetaut, E. Description of the type and referred material of *Phuwiangosaurus sirindhornae* Martin, Buffetaut and Suteethorn, 1994, a sauropod from the Lower Cretaceous of Thailand. *Oryctos* **2**, 39–91 (1999).
14. Allain, R. et al. Un nouveau genre de dinosaure sauropode de la formation des Grès supérieurs (Aptien-Albien) du Laos. *C. R. Acad. Sci.* **329**, 609–616 (1999).
15. Mannion, P. D., Upchurch, P., Jin, X. & Zheng, W. New information on the Cretaceous sauropod dinosaurs of Zhejiang Province, China: Impact on Laurasian titanosauriform phylogeny and biogeography. *R. Soc. Open Sci.* **6**, 191057 (2019).
16. Tong, H., Claude, J., Suteethorn, V., Naksri, W. & Buffetaut, E. Turtle assemblages of the Khorat Group (Late Jurassic-Early Cretaceous) of NE Thailand and their palaeobiogeographical significance. *Geol. Soc. Lond. Spec. Publ.* **315**, 141–152 (2009).

17. Chokchaloemwong, D. et al. A new carcharodontosaurian theropod (Dinosauria: Saurischia) from the Lower Cretaceous of Thailand. *PLoS ONE* **14**, e0222489 (2019).
18. Manitkoon, S. et al. Fossil assemblage from the Khok Pha Suam locality of northeastern, Thailand: An overview of vertebrate diversity from the Early Cretaceous Khok Kruat Formation (Aptian-Albian). *Foss. Rec.* **25**, 83–98 (2022).
19. Manitkoon, S., Deesri, U., Warapeang, P., Nonsrirach, T. & Chanthasit, P. Ornithischian dinosaurs in Southeast Asia: A review with palaeobiogeographic implications. *Foss. Rec.* **26**, 1–25 (2023).
20. Cappetta, H., Buffetaut, E. & Suteethorn, V. A new hybodont shark from the Lower Cretaceous of Thailand. *N. Jahrb. Geol. Palaeontol. Monatsh.* https://doi.org/10.1127/njgpm/1990/1990/659 (1990).
21. Buffetaut, E. et al. The dinosaur fauna from the Khok Kruat Formation (Early Cretaceous) of Thailand. In *Proc. Int. Conf. Geol. Geotechnol. Miner. Resour. Indoch.* 575–581 (2005).
22. Racey, A. & Goodall, J. G. S. Palynology and stratigraphy of the Mesozoic Khorat Group red bed sequences from Thailand. *Geol. Soc. Lond. Spec. Publ.* **315**, 69–83 (2009).
23. Mo, J., Wei, W., Zhitao, H., Xin, H. & Xing, X. A basal titanosauriform from the Early Cretaceous of Guangxi, China. *Acta Geol. Sin. Engl. Ed.* **80**, 486–489 (2006).
24. Mo, J., Xu, X. & Buffetaut, E. A new eusauropod dinosaur from the Lower Cretaceous of Guangxi Province, Southern China. *Acta Geol. Sin. Engl. Ed.* **84**, 1328–1335 (2010).
25. Sekiya, T. *et al.* Sauropod remains from the Khok Kruat Formation, Nakhon Ratchasima Province, northeastern Thailand and implication for the relationship between sauropod tooth morphotype and paleoclimate. in *5th International Symposium on Asian Dinosaurs* 130–132 (Paleontological Lab, Seoul National University, Korea, 2023).
26. Meesook, A. Cretaceous. in *The Geology of Thailand* (eds Ridd, M. F., Barber, A. J. & Crow, M. J.) 169–184 (Geological Society; Distributors, North America, for trade and institutional orders, The Geological Society, c/o AIDC, London: Williston, VT, 2011).
27. Sha, J., Meesook, A. & Nguyen, X. K. Non-marine Cretaceous bivalve biostratigraphy of Thailand, Southern Lao PDR and Central Vietnam. *J. Stratigr.* **36**, 382–399 (2012).
28. Kozu, S. et al. Dinosaur footprint assemblage from the Lower Cretaceous Khok Kruat Formation, Khorat Group, northeastern Thailand. *Geosci. Front.* **8**, 1479–1493 (2017).
29. Cavin, L., Deesri, U. & Suteethorn, V. The Jurassic and Cretaceous bony fish record (Actinopterygii, Dipnoi) from Thailand. *Geol. Soc. Lond. Spec. Publ.* **315**, 125–139 (2009).
30. Deesri, U., Wongko, K. & Cavin, L. Taxic diversity and ecology of Mesozoic bony fish assemblages from the Khorat Group, NE Thailand. *Res. Knowl.* **3**, 18–22 (2017).
31. Cavin, L. et al. A new Lepisosteiformes (Actinopterygii: Ginglymodi) from the Early Cretaceous of Laos and Thailand. *SE Asia. J. Syst. Palaeontol.* **17**, 393–407 (2019).
32. Yabe, H. & Obata, T. On some fossil fishes from the Cretaceous of Japan. *Jpn. J. Geol. Geogr.* **8**, 1–8 (1930).
33. Cappetta, H., Buffetaut, E., Cuny, G. & Suteethorn, V. A new Elasmobranch assemblage from the Lower Cretaceous of Thailand. *Palaeontology* **49**, 547–555 (2006).
34. Cuny, G., Suteethorn, V., Kamha, S. & Buffetaut, E. Hybodont sharks from the Lower Cretaceous Khok Kruat Formation of Thailand, and hybodont diversity during the Early Cretaceous. *Geol. Soc. Lond. Spec. Publ.* **295**, 93–107 (2008).
35. Cuny, G. et al. New data on Cretaceous freshwater hybodont sharks from Guangxi Province. *South China. Res. Knowl.* **3**, 11–15 (2017).
36. Tong, H., Suteethor, V., Claude, J., Buffetaut, E. & Jintasakul, P. The turtle fauna from the Khok Kruat Formation (Early Cretaceous) of Thailand. in *Proceedings of the International Conference on Geology, Geotechnology and Mineral Resources of Indochina* 610–6144 (Khon Kaen University, Khon Kaen, 2005).
37. Lauprasert, K., Cuny, G., Thirakhupt, K. & Suteethorn, V. *Khoratosuchus jintasakuli* gen. et sp. nov., an advanced neosuchian crocodyliform from the Early Cretaceous (Aptian-Albian) of NE Thailand. *Geol. Soc. Lond. Spec. Publ.* **315**, 175–187 (2009).
38. Lauprasert, K. et al. Atoposaurid crocodyliforms from the Khorat Group of Thailand: First record of Theriosuchus from Southeast Asia. *Paläontol. Z.* **85**, 37–47 (2011).
39. Manitkoon, S. et al. First gnathosaurine (Pterosauria, Pterodactyloidea) from the Early Cretaceous of eastern Thailand. *Cretac. Res.* https://doi.org/10.1016/j.cretres.2025.106135 (2025).
40. Nakamura, T. et al. New pterosaur fossils from the Khok Kruat Formation, Nakhon Ratchasima, Thailand. in *The 6th International Palaeontological Congress (Khon Kaen, Thailand)* vol. 206 199 (Thailand, 2022).
41. Buffetaut, E. & Suteethorn, V. A new iguanodontian dinosaur from the Khok Kruat Formation (Early Cretaceous, Aptian) of Northeastern Thailand. *Ann. Paléontol.* **97**, 51–62 (2011).
42. Shibata, M., Jintasakul, P. & Azuma, Y. A new Iguanodontian dinosaur from the Lower Cretaceous Khok Kruat Formation, Nakhon Ratchasima in Northeastern Thailand. *Acta Geol. Sin. - Engl. Ed.* **85**, 969–976 (2011).
43. Shibata, M., Jintasakul, P., Azuma, Y. & You, H.-L. A new basal Hadrosauroid dinosaur from the Lower Cretaceous Khok Kruat Formation in Nakhon Ratchasima Province, Northeastern Thailand. *PLoS ONE* **10**, e0145904 (2015).
44. Chokchaloemwong, D., Hattori, S., Yukawa, H., Shibata, M. & Naksri, W. A new ornithomimosaurian material from the Khok Kruat Formation, Lower Cretaceous of Thailand. *Mem. Fukui Prefect. Dinosaur Mus.* **23**, 1–7 (2024).
45. Khansubha, S., Pothichaiya, C., Rugbumrung, M. & Meesook, A. The Gigantic Titanosauriform Sauropod from the Early Cretaceous Khok Kruat Formation in the Northeastern of Thailand: A Preliminary Report. in vol. Program and Abstracts 141–142 (Journal of Vertebrate Paleontology, 2017).
46. Meesook, A. *The Cretaceous Giant Sauropod from the Khok Kruat Formation at Ban Pha Nang Sua, Nong Bua Rawe District, Chaiyaphum Province, Northeastern Thailand: A Preliminary Report*. (Division of Fossil Protection, Department of Mineral Resources Thailand, 2016).
47. Wilson, J. A. & Sereno, P. C. Early evolution and higher-level phylogeny of sauropod dinosaurs. *J. Vertebr. Paleontol.* **18**, 1–79 (1998).
48. Suteethorn, S. et al. A new skeleton of *Phuwiangosaurus sirindhornae* (Dinosauria, Sauropoda) from NE Thailand. *Geol. Soc. Lond. Spec. Publ.* **315**, 189–215 (2009).
49. Suteethorn, S., Le Loeuff, J., Buffetaut, E. & Suteethorn, V. Description of topotypes of *Phuwiangosaurus sirindhornae*, a sauropod from the Sao Khua Formation (Early Cretaceous) of Thailand, and their phylogenetic implications. *N. Jahrb. Geol. Palaeontol. Abh.* https://doi.org/10.1127/0077-7749/2010/0036 (2010).
50. Poropat, S. F. et al. New Australian sauropods shed light on Cretaceous dinosaur palaeobiogeography. *Sci. Rep.* **6**, 34467 (2016).
51. Carballido, J. L., Salgado, L., Pol, D., Canudo, J. I. & Garrido, A. A new basal rebbachisaurid (Sauropoda, Diplodocoidea) from the Early Cretaceous of the Neuquén Basin; evolution and biogeography of the group. *Hist. Biol.* **24**, 631–654 (2012).
52. Li, L.-G., Li, D.-Q., You, H.-L. & Dodson, P. A new titanosaurian sauropod from the Hekou Group (Lower Cretaceous) of the Lanzhou-Minhe Basin, Gansu Province, China. *PLoS ONE* **9**, e85979 (2014).
53. Díez Díaz, V., Pereda Suberbiola, X. & Sanz, J. Appendicular skeleton and dermal armour of the Late Cretaceous titanosaur *Lirainosaurus astibia* (Dinosauria: Sauropoda) from Spain. *Palaeontol. Electron.* **19**, 18 (2013).
54. Zaher, H. et al. A complete skull of an Early Cretaceous sauropod and the evolution of advanced titanosaurians. *PLoS ONE* **6**, e16663 (2011).
55. You, H.-L., Li, D.-Q., Zhou, L.-Q. & Ji, Q. *Daxiatitan binglingi*: A giant sauropod dinosaur from the Early Cretaceous of China. *Gansu Geol.* **17**, 1–10 (2008).

56. Lü, J. et al. A preliminary report on the new dinosarian fauna from the Cretaceous of the Ruyang Basin, Henan Province of Central China. *J. Paleontol. Soc. Korea* **25**, 43–56 (2009).
57. Lü, J. et al. *Osteological Study of the Giant Sauropod Dinosaur:* Ruyangosaurus (Lü et al., 2009). (Geological Publishing House, 2014).
58. Carballido, J. L. & Sander, P. M. Postcranial axial skeleton of *Europasaurus holgeri* (Dinosauria, Sauropoda) from the Upper Jurassic of Germany: Implications for sauropod ontogeny and phylogenetic relationships of basal Macronaria. *J. Syst. Palaeontol.* **12**, 335–387 (2014).
59. He, X., Li, K. & Cai, K. The middle Jurassic dinosaur fauna from Dashanpu, Zigong, Sichuan. In *Omeisaurus tianfuensis* Vol. vol. 4 1–143 (Sichuan Publishing House of Science and Technology, 1988).
60. Wilson, J. A., D'Emic, M. D., Ikejiri, T., Moacdieh, E. M. & Whitlock, J. A. A nomenclature for vertebral fossae in sauropods and other saurischian dinosaurs. *PLoS ONE* **6**, e17114 (2011).
61. Whitlock, J. A. A phylogenetic analysis of Diplodocoidea (Saurischia: Sauropoda). *Zool. J. Linn. Soc.* **161**, 872–915 (2011).
62. Carballido, J. L., Pol, D., Cerda, I. & Salgado, L. The osteology of *Chubutisaurus insignis* del Corro, 1975 (Dinosauria: Neosauropoda) from the 'middle' Cretaceous of central Patagonia, Argentina. *J. Vertebr. Paleontol.* **31**, 93–110 (2011).
63. Wang, X. et al. *Dongbeititan dongi*, the first sauropod dinosaur from the Lower Cretaceous Jehol Group of Western Liaoning Province, China. *Acta Geol. Sin. Engl. Ed.* **81**, 911–916 (2007).
64. Torcida Fernández-Baldor, F., Canudo, J. I., Huerta, P., Moreno-Azanza, M. & Montero, D. *Europatitan eastwoodi*, a new sauropod from the Lower Cretaceous of Iberia in the initial radiation of somphospondylans in Laurasia. *PeerJ* **5**, e3409 (2017).
65. Canudo, J. I., Royo-Torres, R. & Cuenca-Bescós, G. A new sauropod: *Tastavinsaurus sanzi* gen. et sp. nov. from the Early Cretaceous (Aptian) of Spain. *J. Vertebr. Paleontol.* **28**, 712–731 (2008).
66. Wilson, J. A. & Allain, R. Osteology of *Rebbachisaurus garasbae* Lavocat, 1954, a diplodocoid (Dinosauria, Sauropoda) from the early Late Cretaceous–aged Kem Kem beds of southeastern Morocco. *J. Vertebr. Paleontol.* **35**, e1000701 (2015).
67. Gorscak, E. et al. A new titanosaurian (Dinosauria: Sauropoda) from the Upper Cretaceous (Campanian) Quseir Formation of the Kharga Oasis, Egypt. *J. Vertebr. Paleontol.* **42**, e2199810 (2022).
68. Lacovara, K. J. et al. A gigantic, exceptionally complete titanosaurian sauropod dinosaur from Southern Patagonia, Argentina. *Sci. Rep.* **4**, 6196 (2014).
69. Hatcher, J. B. A new name for the dinosaur *Haplocanthus* Hatcher. *Proc. Biol. Soc. Wash.* **16**, 100 (1903).
70. Osborn, H. F. & Mook, C. C. *Camarasaurus, Amphicoelias*, and other sauropods of Cope. in *Memoirs of the American Museum of Natural History* vol. V. 3, Pt. 3 243–491 (American Museum of Natural History, New York, 1921)
71. Janensch, W. Die Wirbelsäule von *Brachiosaurus brancai*. in *Wissenschaftliche Ergebnisse der Tendaguru-Expedition 1909-1912* 27–93 (E. Schweizerbart'sche Verlagsbuchhandlung, Berlin, 1950).
72. Dai, H. et al. New macronarian from the Middle Jurassic of Chongqing, China: Phylogenetic and biogeographic implications for neosauropod dinosaur evolution. *R. Soc. Open Sci.* **9**, 220794 (2022).
73. Lü, J., Yoichi, A., Rongjun, C., Wenjie, Z. & Xingsheng, J. A new titanosauriform sauropod from the early late cretaceous of dongyang, zhejiang province. *Acta Geol. Sin. Engl. Ed.* **82**, 225–235 (2008).
74. D'Emic, M. D. et al. Osteology of *Huabeisaurus allocotus* (Sauropoda: Titanosauriformes) from the Upper Cretaceous of China. *PLoS ONE* **8**, e69375 (2013).
75. Carballido, J. L. et al. A new giant titanosaur sheds light on body mass evolution among sauropod dinosaurs. *Proc. R. Soc. B Biol. Sci.* **284**, 20171219 (2017).
76. Beeston, S. L. et al. Reappraisal of sauropod dinosaur diversity in the Upper Cretaceous Winton Formation of Queensland, Australia, through 3D digitisation and description of new specimens. *PeerJ* **12**, e17180 (2024).
77. Wilson, J. A. & Upchurch, P. A revision of *Titanosaurus* Lydekker (dinosauria–sauropoda), the first dinosaur genus with a 'Gondwanan' distribution. *J. Syst. Palaeontol.* **1**, 125–160 (2003).
78. Young, C. C. Dinosaurian remains from Mengyin. *Shantung. Bull. Geol. Soc. China* **14**, 519–534 (1935).
79. Tschopp, E., Mateus, O. & Benson, R. B. J. A specimen-level phylogenetic analysis and taxonomic revision of Diplodocidae (Dinosauria, Sauropoda). *PeerJ* **3**, e857 (2015).
80. Gonzalez Riga, B. J. A new titanosaur (Dinosauria, Sauropoda) from the Upper Cretaceous of Mendoza. *Argentina. Amehginiana* **4**, 155–172 (2003).
81. Wilson, JeffreyA. Sauropod dinosaur phylogeny: Critique and cladistic analysis. *Zool. J. Linn. Soc.* **136**, 215–275 (2002).
82. Azuma, Y. & Shibata, M. *Fukuititan nipponensis*, a new titanosauriform sauropod from the Early Cretaceous Tetori Group of Fukui Prefecture, Japan. *Acta Geol. Sin. Engl. Ed.* **84**, 454–462 (2010).
83. Borsuk-Bialynicka, M. A new camarasaurid sauropod *Opisthocoelicaudia skarzynskii* gen. n., sp. n. from the Upper Cretaceous of Mongolia. *Palaeontol. Pol.* **37**, 5–64 (1977).
84. Otero, A. Forelimb musculature and osteological correlates in Sauropodomorpha (Dinosauria, Saurischia). *PLoS ONE* **13**, e0198988 (2018).
85. Upchurch, P., Mannion, P. D. & Taylor, M. P. The anatomy and phylogenetic relationships of "*Pelorosaurus becklesii*" (Neosauropoda, Macronaria) from the Early Cretaceous of England. *PLoS ONE* **10**, e0125819 (2015).
86. Mo, J.-Y., Fu, Q.-Y., Yu, Y.-L. & Xu, X. A new titanosaurian sauropod from the Upper Cretaceous of Jiangxi Province, Southern China. *Hist. Biol.* **0**, 1–15 (2023).
87. Saegusa, H. & Ikeda, T. A new titanosauriform sauropod (Dinosauria: Saurischia) from the Lower Cretaceous of Hyogo, Japan. *Zootaxa* **3848**, 1–66 (2014).
88. Lehman, T. M. & Coulson, A. B. A juvenile specimen of the sauropod dinosaur *Alamosaurus sanjuanensis* from the Upper Cretaceous of Big Bend National Park, Texas. *J. Paleontol.* **76**, 156–172 (2002).
89. Sereno, P. C. et al. Structural extremes in a cretaceous dinosaur. *PLoS ONE* **2**, e1230 (2007).
90. Mocho, P. et al. New sauropod dinosaur from the Lower Cretaceous of Morella (Spain) provides new insights on the evolutionary history of Iberian somphospondylan titanosauriforms. *Zool. J. Linn. Soc.* **201**, 214–268 (2024).
91. Díez Díaz, V., Mannion, P. D., Csiki-Sava, Z. & Upchurch, P. Revision of Romanian sauropod dinosaurs reveals high titanosaur diversity and body-size disparity on the latest Cretaceous Hațeg Island, with implications for titanosaurian biogeography. *J. Syst. Palaeontol.* **23**, 2441516 (2025).
92. Klein, N., Sander, M. & Suteethorn, V. Bone histology and its implications for the life history and growth of the Early Cretaceous titanosaur *Phuwiangosaurus sirindhornae*. *Geol. Soc. Lond. Spec. Publ.* **315**, 217–228 (2009).
93. Kaikaew, S., Suteethorn, V., Deesri, U. & Suteethorn, S. The endocast of *Phuwiangosaurus sirindhornae* from the Lower Cretaceous of Thailand. *Cretac. Res.* **144**, 105434 (2023).
94. Mo, J. et al. New fossil remains of *Fusuisaurus zhaoi* (Sauropoda: Titanosauriformes) from the Lower Cretaceous of Guangxi, southern China. *Cretac. Res.* **109**, 104379 (2020).
95. Shan, B. The re-description of *Liaoningotitan sinensis* Zhou et al., 2018. *PeerJ* **13**, e19154 (2025).
96. Canudo, J. I., Ruiz-Omeñaca, J. I., Barco, J. L. & Royo-Torres, R. ¿Saurópodos asiáticos en el Barremiense inferior (Cretácico Inferior) de España?. *Ameghiniana* **39**, 443–452 (2002).
97. Dieudonné, P.-E., Tortosa, T., Fernández-Baldor, F. T., Canudo, J. I. & Díaz-Martínez, I. An unexpected early rhabdodontid from Europe (Lower Cretaceous of Salas de los Infantes, Burgos Province, Spain) and a re-examination of basal iguanodontian relationships. *PLoS ONE* **11**, e0156251 (2016).

98. Escanero-Aguilar, D., Torcida Fernández-Baldor, F., Pereda-Suberbiola, X. & Huerta, P. Skull material of an Early Cretaceous hadrosauriform dinosaur (Ornithopoda) from Salas de los Infantes (Burgos, Spain). *J. Iber. Geol.* **50**, 67–82 (2024).
99. Sander, P. M. et al. Biology of the sauropod dinosaurs: The evolution of gigantism. *Biol. Rev.* **86**, 117–155 (2011).
100. Sander, P. M. An evolutionary cascade model for sauropod dinosaur gigantism—overview. *Update and Tests. PLOS ONE* **8**, e78573 (2013).
101. Benson, R. B. J. et al. Rates of dinosaur body mass evolution indicate 170 million years of sustained ecological innovation on the avian stem lineage. *PLOS Biol.* **12**, e1001853 (2014).
102. D'Emic, M. D. The evolution of maximum terrestrial body mass in sauropod dinosaurs. *Curr. Biol.* **33**, R349–R350 (2023).
103. Souza, L. M. & Santucci, R. M. Body size evolution in Titanosauriformes (Sauropoda, Macronaria). *J. Evol. Biol.* **27**, 2001–2012 (2014).
104. Benson, R. B. J., Hunt, G., Carrano, M. T. & Campione, N. Cope's rule and the adaptive landscape of dinosaur body size evolution. *Palaeontology* **61**, 13–48 (2018).
105. González Riga, B. J., Lamanna, M. C., Ortiz David, L. D., Calvo, J. O. & Coria, J. P. A gigantic new dinosaur from Argentina and the evolution of the sauropod hind foot. *Sci. Rep.* **6**, 19165 (2016).
106. Xu, X., Zhang, X., Tan, Q., Zhao, X. & Tan, L. A new titanosaurian sauropod from late cretaceous of Nei Mongol, China. *Acta Geol. Sin. Engl. Ed.* **80**, 20–26 (2006).
107. Sewall, J. O. et al. Climate model boundary conditions for four Cretaceous time slices. *Clim. Past* **3**, 647–657 (2007).
108. Upchurch, P. & Chiarenza, A. A. A brief review of non-avian dinosaur biogeography: State-of-the-art and prospectus. *Biol. Lett.* **20**, 20240429 (2024).
109. Chiarenza, A. A., Mannion, P. D., Farnsworth, A., Carrano, M. T. & Varela, S. Climatic constraints on the biogeographic history of Mesozoic dinosaurs. *Curr. Biol.* **32**, 570-585.e3 (2022).
110. Chiarenza, A. A. The macroecology of Mesozoic dinosaurs. *Biol. Lett.* **20**, 20240392 (2024).
111. Heimhofer, U. et al. Vegetation response to exceptional global warmth during Oceanic Anoxic Event 2. *Nat. Commun.* **9**, 3832 (2018).
112. Noto, C. R. & Grossman, A. Broad-scale patterns of late jurassic dinosaur paleoecology. *PLoS ONE* **5**, e12553 (2010).
113. Goloboff, P. A. & Morales, M. E. TNT version 1.6, with a graphical interface for MacOS and Linux, including new routines in parallel. *Cladistics* **39**, 144–153 (2023).
114. Goloboff, P. A. Extended implied weighting. *Cladistics* **30**, 260–272 (2014).
115. Goloboff, P. A., Torres, A. & Arias, J. S. Weighted parsimony outperforms other methods of phylogenetic inference under models appropriate for morphology. *Cladistics* **34**, 407–437 (2018).
116. Ezcurra, M. D. Exploring the effects of weighting against homoplasy in genealogies of palaeontological phylogenetic matrices. *Cladistics* **40**, 242–281 (2024).
117. Ramanujan, S. Modular equations and approximations to π. *Q. J. Math.* **45**, 350–372 (1914).
118. Kitchener, J. L., Campione, N. E., Smith, E. T. & Bell, P. R. High-latitude neonate and perinate ornithopods from the mid-Cretaceous of southeastern Australia. *Sci. Rep.* **9**, 19600 (2019).
119. Redelstorff, R., Hübner, T. R., Chinsamy, A. & Sander, P. M. Bone histology of the stegosaur *Kentrosaurus aethiopicus* (Ornithischia: Thyreophora) from the Upper Jurassic of Tanzania. *Anat. Rec.* **296**, 933–952 (2013).
120. Cooper, L. N., Lee, A. H., Taper, M. L. & Horner, J. R. Relative growth rates of predator and prey dinosaurs reflect effects of predation. *Proc. R. Soc. B Biol. Sci.* **275**, 2609–2615 (2008).
121. Seebacher, F. A new method to calculate allometric length-mass relationships of dinosaurs. *J. Vertebr. Paleontol.* **21**, 51–60 (2001).
122. Wikimedia Commons contributors. File:Thailand Chaiyaphum locator map.svg. Wikimedia Commons, https://commons.wikimedia.org/w/index.php?title=File:Thailand_Chaiyaphum_locator_map.svg&oldid=956503538 (2024).
123. Hongsabal, N. *Geological Map of Northeastern Thailand* (Department of Mineral Resources, 2023).

Acknowledgements

We would like to thank Cherdchan Pothichaiya (Mineral Resource Regional Office 2, DMR2), Chandech Jantarat (Geological Survey Division), Mana Rugbumrung (Fossil Conservation Division), and Sathit Saratan (Sirindhorn Museum) along with other staff and volunteers at the Sirindhorn Museum, Mineral Resource Office 2 (DMR2), Fossil Conservation Division, Department of Mineral Resources, Palaeontological Research and Education Centre, Mahasarakham University, Nong Bua Rawe Subdistrict Municipality Office, as well as participants of Paleo Camp 2024, who took part in investigations and excavations at the Ban Pha Nang Sua locality from 2016 to 2024 including those who prepared and made molds and casts of the specimens. We also thank Sawad Luangnan for her care and maintenance of the facilities and excavation site at the Ban Pha Nang Sua locality from 2016 to the present. We would also like to thank Sakboworn Tumpeesuwan and Wongwech Chowchuvech for providing data on bivalves and theropods, as well as Patchanop Boonsai, Chatcharin Somboon, and Matus Charoenjit (Facebook Fanpage: DinoThaiThai) for kindly providing their artwork. We are also grateful to our reviewers, Pedro Mocho and an anonymous reviewer, whose comments improved this contribution. We acknowledge the Willi Hennig Society, which has sponsored the development and free distribution of TNT. Finally, we would like to dedicate this research to the late Dr. Assanee Meesook who first surveyed and described the geology of Ban Pha Nang Sua and the late Thanom Luangnan, who discovered the Nagatitan holotype.

Author contributions

TS conceived and designed the experiments, performed the experiments, analysed and interpreted the data, produced figures and tables and led the writing of the manuscript. SK conceived and designed the experiments, involved in and supervised fieldwork, performed the experiments, analysed and interpreted the data, produced figures and tables, contributed to drafts of the manuscript and approved the final manuscript. SM facilitated 3D surface scanning of specimens, involved in and supervised fieldwork, interpreted the data, produced figures, contributed to drafts of the manuscript and approved the final manuscript. RH involved in and supervised fieldwork, interpreted the data, contributed to drafts of the manuscript and approved the final manuscript. PDM conceived and designed the experiments, analysed and interpreted the data, contributed to drafts of the manuscript and approved the final manuscript. PU conceived and designed the experiments, interpreted the data, contributed to drafts of the manuscript and approved the final manuscript.

Funding

The contributions of SM and TS were supported by a National Geographic Society grant (EC-106536R-24) for

fieldwork and laboratory analysis. Additional financial support was also provided by Mahasarakham University, and the Geological Society of Thailand. PDM's research was supported by funding from The Royal Society (UF160216, URF\R\221010).

Declarations

Competing interests

The authors declare no competing interests.

Additional information

Supplementary Information The online version contains supplementary material available at https://doi.org/10.1038/s41598-026-47482-x.

Correspondence and requests for materials should be addressed to S.M.

Reprints and permissions information is available at www.nature.com/reprints.

Publisher's note Springer Nature remains neutral with regard to jurisdictional claims in published maps and institutional affiliations.